Faculdade de Engenharia da Universidade do Porto
Instituto de Ciências Biomédicas

Master Dissertation

Development of Nanoparticle-in-Microparticle systems for oral delivery of triptorelin

Author

Ana Rita Salgado Ribeiro

Supervisor
Bruno Sarmento, PhD

Co-supervisor
Francisca Araújo, PhD

DISSERTATION FOR THE DEGREE OF MASTER OF SCIENCE IN BIOENGINEERING AT FACULDADE DE ENGENHARIA DA UNIVERSIDADE DO PORTO AND INSITUTO DE CIÊNCIAS BIOMÉDICAS ABEL SALAZAR

February 2018

U.PORTO
FEUP FACULDADE DE ENGENHARIA
UNIVERSIDADE DO PORTO

INSTITUTO DE INVESTIGAÇÃO
E INOVAÇÃO EM SAÚDE
UNIVERSIDADE DO PORTO

U.PORTO
INSTITUTO DE CIÊNCIAS BIOMÉDICAS ABEL SALAZAR
UNIVERSIDADE DO PORTO

Development of Nanoparticle-in-Microparticle systems for oral delivery of triptorelin

Ana Rita Salgado Ribeiro

Dissertation
for the Degree of Master of Science in Bioengineering,
at Faculdade de Engenharia da Universidade do Porto
and Instituto de Ciências Biomédicas Abel Salazar

Supervisor: Bruno Sarmento, PhD
Co-supervisor: Francisca Araújo, PhD

February 2018

invent yourself and then reinvent yourself,
don't swim in the same slough.
invent yourself and then reinvent yourself
and
stay out of the clutches of mediocrity.

invent yourself and then reinvent yourself,
change your tone and shape so often that they can
never
categorize you.

reinvigorate yourself and
accept what is
but only on the terms that you have invented
and reinvented.

be self-taught.

and reinvent your life because you must;
it is your life and
its history
and the present
belong only to
you.

Charles Bukowski

Acknowledgments

To the three generations of women in my house. Maria Helena, Ana Sofia and Luz Batista. To them, for being the strongest women I know, my core and the ultimate love of my life. For all the support, the patience, and mainly, the greatest example they always were to me.

Secondly, to Patrick J. O'Neill, the most caring man I could have wished to have around during this journey. Thank you for always bringing joy to my days. Mo chroi, mo chuisle.

A heartfelt thanks to Prof. Bruno Sarmento and Dr. Francisca Araújo, for the great opportunity of working in a multidisciplinary laboratory, for continuously supervising my work while giving me space to make my project, truly my project. Was a privilege to have the chance to work in a group where scientific discussions are permanently instigated. I am grateful to everyone in Nanomedicines and Translational Drug Delivery group for the insightful opinions and for teaching me so much.

To Ferring Pharmaceuticals for giving me the opportunity to work in this project. It was a great privilege to have a MSc thesis developed in such close contact with a pharmaceutical company that is in the forefront of biotechnology innovation. I am very grateful for this opportunity and proud to have been involved in a project with recognized translational potential to clinic.

To Virgínia Gonçalves for always being so helpful and so kind to me.

To Carlos Fernandes for all the patience and the availability to discuss science with me, and mainly, for the valuable contributions given for this work.

To Prof. Paul Shiels, for giving me the most amazing opportunity of doing an internship in his lab during my MSc, where I learnt and grew so much both on an academic level and a personal level. In WWRCR I had Alan McIntyre helping me, for whom I have great gratitude. Not

only for teaching me all the techniques and always being available to help me but mostly, for always trusting my work. This experience and the great people I shared it with were a turning point in my life as it gave me the confidence and motivation I lacked and boosted my critical sense and autonomy in the lab, without which, I would not be able to conduct the work here presented.

To Mariana Neves with all my heart, the best friend I had in these years and my greatest motivation to finish my MSc.

A heart-warming thanks to my second family, most of which I met and kept around since the first year of my life; Manuel Semedo, Pedro Oliveira, Francisco Gama, Nuno Santiago, Henrique Carvalho, Rita Raposo, Ricardo Cruz, Daniela Simões, Ana Maria, Catarina Marques, Pedro Veiga, Filipa Santos. For being by my side always. For the never-ending happy memories we have, and for the ones yet to come. I was blessed with best friends there are, and I was lucky to spend all my life with them.

Finally, to FEUP, ICBAS and i3s for receiving me and providing me all the physical resources and giving me the chance to learn from great professors during this journey.

Agradecimentos

Às três gerações de mulheres da minha casa. Maria Helena, Ana Sofia e Luz Batista.

A elas, por serem as mulheres mais fortes que conheço, o meu núcleo forte e o grande amor da minha vida. Por todo o apoio, paciência e sobretudo, por terem sido sempre o maior exemplo que poderia ter tido. Obrigada.

De seguida, ao Patrick J. O'Neill o homem mais carinhoso que poderia desejar ter ao meu lado durante este percurso. Obrigada por trazeres sempre alegria aos meus dias. Mo chroi, mo chuisle.

Ao Prof. Bruno Sarmento e Dr. Francisca Araújo, pela oportunidade de trabalhar num laboratório multidisciplinar, pela supervisão continua do meu trabalho, mas sempre dando-me margem para fazer do meu projeto, de facto, um projeto meu. Foi um privilégio poder trabalhar num grupo onde a discussão cientifica é continuamente instigada. Obrigada a todos os que constituem o grupo "Nanomedicines and Translational Medicine" pelas opiniões construtivas e pela a aprendizagem continua.

À Ferring Pharmaceuticals por me ter dado a oportunidade de trabalhar neste projecto. Foi um privilégio ter uma tese de mestrado desenvolvida em contacto com uma companhia farmacêutica que está na vanguarda da inovação em biotecnologia. Estou muito grata pela oportunidade e orgulhosa de ter participado num projecto com potencial reconhecido de translação para a clínica.

À Virgínia Gonçalves pela simpatia e disponibilidade constantes, sobretudo nesta fase final.

Ao Carlos Fernandes, por toda a paciência e pelas discussões produtivas, mas sobretudo, pelo contributo valioso para este trabalho.

Ao Prof. Paul Shiels, por me ter dado a incrível oportunidade de fazer um estágio no seu laboratório, onde aprendi e cresci muito, tanto em termos académicos com pessoais. Neste período, tive a sorte de ter o Alan McIntyre a ajudar-me, e por isso estou muito grata. Não apenas pelos conhecimentos técnicos que me passou e por estar sempre tão disponível, mas sobretudo por ter confiado sempre no meu trabalho. Esta experiência e as pessoas com quem a partilhei foram um ponto de viragem na minha vida. Aqui ganhei a confiança e motivação que não tive durante o curso, desenvolvi o meu espirito crítico e a minha autonomia no laboratório. Sem estas capacidades, não creio que tivesse sido capaz de desenvolver o trabalho aqui apresentado.

À Mariana Neves com todo o meu coração; a melhor amiga que tive nestes anos e a minha grande motivação para terminar o MSc.

Um gigante obrigada aos que considero como minha segunda família e que me acompanham desde o primeiro ano da minha vida. Manuel Semedo, Pedro Oliveira, Francisco Gama, Nuno Santiago, Henrique Carvalho, Rita Raposo, Ricardo Cruz, Daniela Simões, Ana Maria, Catarina Marques, Pedro Veiga, Filipa Santos. Por estarem sempre comigo. Os melhores amigos que poderia ter e com quem tive a sorte de partilhar toda a minha vida.

Finalmente, à FEUP, ao ICBAS e ao i3s; pelos excelentes professores e por todos os recursos disponibilizados durante esta jornada, que me permitiram uma aprendizagem contínua.

- this page was intentionally left in blank -

Abstract

The development of nanosystems for drug delivery has raised great interest in the past few decades. More specifically, these systems seem to have great potential in aiding the improvement of bioavailability of proteins and peptide administered through oral route instead of more invasive ways of administration. Considering this, the goal set for this project was the development of Nanoparticle-in-Microparticle systems for the oral delivery of a model peptide (Triptorelin), that presented both gastroresistant and mucodiffusive properties.

The approach used was the encapsulation of triptorelin by double-emulsion method in polymeric nanoparticles (NPs). PLGA was the selected polymer for the purpose due to its biodegradability and biocompatibility and for being widely used for drug delivery applications. Here, we were able to attain a drug loading of 2.59%. As this value is not very high, it does not compromise the colloidal properties of the NPs. The average size of the NPs was in the range of 200 nm, being highly monodisperse and negatively charged, as expected. After conjugation with polyethylene glycol and chitosan (mPEG-CS) the polydispersion index remained low, but size increased slightly, and the overall charge of the NPs turn neutral, as a reflection of the presence of the positive amines of CS on the surface of NPs. These results were highly reproducible between batches and hence we proceeded to downstream analysis of the formulations *in vitro*. Firstly, the safety potential of the formulation was assessed by metabolic activity assays in Caco-2 and HT29MTX cell lines. Here we observed that mPEG-CS-PLGA loaded NPs did not induce a decrease of metabolic activity of cells when compared to the controls, suggesting its safety.

Regarding permeability assays, it was observed that the system did not present the properties intended as the peptide did not show an increased permeation of the monolayer when encapsulated in the modified PLGA NPs. This is probably related to the slow degradation of PLGA which strongly delays the peptide release. Here, other factors need to be considered, namely the mucodiffusive properties of the formulation, which were not assessed, and we cannot confirm if the modification effectively promoted a closer contact to the cells.

Simultaneously with *in vitro* analysis, the NPs were encapsulated in microparticles to provide the gastroresistant structure of the NiM systems. To do so, hydroxypropyl methyl celullose acetate succinate (HPMC-AS) was the selected enteric polymer as it keeps its integrity for acidic conditions, suffering dissolution for pH ≥ 6, which has been reported to be the

physiological conditions of the small intestine. Here is where absorption occurs and hence, where the NPs must be released.

The dissolution profile of the microparticles under incubation with different pH buffers was assessed and the results corroborated its potential as a gastroresistant structure, as no microparticles remained intact after incubation with buffer at pH 6.

- this page was intentionally left in blank -

Table of Contents

Abbreviation & Acronyms List

AE – Association Efficiency

AF – Amicon Filters

AW – After wash

ART – Assisted Reproductive Therapy

BW – Before wash

CS – Chitosan

D_2O – Deuterated water

DA – Degree of acetylation

DD – Degree of deacetylation

DL – Drug loading

DLS – Dynamic Light Scattering

DMEM – Dulbecco's Modified Eagle Medium

DMSO – Dimethyl sulfoxide

EDC – 1-ethyl-3-(-3-dimethylaminopropyl) carbodiimide

EMA – European Medicines Agency

FDA – Food and Drug Administration

FSH – Follicule Stimulating Hormone

GI – Gastrointestinal

GnRH – Gonadotropin-Releasing Hormone

HBSS - Hank’s balanced salt solution

HPLC – High Performance Liquid Chromatography

HPMC-AS – Hydroxypropyl methyl celullose Acetate Succinate

i.v. - Intravenous

LH – Luteneizing Hormone

LMW – Low molecular weight

mQH_2O – MiliQ water

MES - 2-(N-morpholino)ethanesulfonic acid

mPEG – Methoxypoly (ethylene glycol)

MPs – Microparticles

MTT – 3-(4,5-dimethylthiazol-2-yl)-2,5-diphenyltetrazolium bromide

NTA – Nanoparticle Tracking Analysis

NHS – N-hydroxysuccinimide

NiM – Nanoparticle-in-microparticle

NMR – Nuclear Magnetic Resonance

NPs – Nanoparticles

PBS – Phosphate Buffered Saline

PEG – Polyethylene glycol

PLGA – Poly(lactic-co-glycolic acid)

PVA – Polyvinyl alcohol

SD – Susbtitution Degree

SEM – Scanning Electron Microscope

TEA – Triethylamine

TEAP – Triethylammonium phosphate buffer

TEER – Transepithelial Electrical Resistance

TEM – Transmission Electron Microscopy

THF – Tetrahydrofuran

UC – Ultra centrifugation

List of figures

List of tables

- this page was intentionally left in blank -

Chapter 1

OULINE

1.1. Objective and rationale of the work

Research in nanotechnology field applied to health sciences has been gaining great relevance for the past decades, namely for drug delivery proposes. The increased interest arises from the possibility of changing the properties of the formulation such as the solubility of the molecule, its controlled release or targeting to specific site of action [1]. All these parameters can be tuned and adjusted for the treatment of numerous pathologies, thus presenting great potential in therapeutic applications.

Proteins and small peptides are extensively used in clinics in the treatment of numerous diseases, due to their high selectivity and potent action [2]. However, unlike small molecule drugs, the development of formulations with these biomolecules is highly dependent on the alteration of their properties. For instance, these biomolecules cannot be administered through oral route in its free form, due to low bioavailability resulting from enzymatic degradation and poor penetration in the intestinal membrane [3]. Yet, as the oral route is by far the most widely used route of administration, due to high patience compliance, much research has been performed towards that aim. Hence, the main goal of this project is the development of a gastroresistant and mucodiffusive Nanoparticle-in-Microparticle (NiM) system for oral delivery of a decapeptide, triptorelin (Trp). This drug is an analogue of Gonadotropin-Releasing Hormone (GnRH) currently on the market, used for prostate cancer treatment and it is administered through subcutaneous or intramuscular injection. Parenteral routes of administration are highly invasive resulting in very low patient compliance. Thus, the development of a gastroresistant and mucodiffusive system would allow the administration of this drug through oral route.

Overall, the rationale behind this work is that a new versatile system can be produced for the oral delivery of proteins and peptides and it can be produced as an alternative to more invasive routes of administration, resulting in higher patient compliance. If proven successful, this NiM system could highly impact and improve patients lives as it would simplify an

autonomous administration of drugs while minimizing risks of potential local infections that are associated to parenteral routes.

The specific objectives of this dissertation are:

i. To produce and characterize Trp loaded nanoparticles (NPs), with surface modification to confer mucodiffusive properties to the final formulation.
ii. To microencapsulate the NPs into gastroresistant structures, to assure the protection of the overall structure of NPs and encapsulated peptide.
iii. To assess the safety of the system when in contact with relevant cell lines with intestinal origin.
iv. To perform permeability studies to evaluate the impact of the mucodiffusive modification of NPs on drug permeation through relevant i*n vitro* intestinal models.

1.2. Structure of dissertation

This work is divided in four main chapters. In the first one – Outline, the context, rationale and structure of the dissertation is presented. In Chapter 2 – Literature Review, there is a review of literature to enlighten the reader about the current state of art the of nanotechnologies applied to drug delivery. Chapter 3 – Materials and Methods describes the materials used and the experiments performed. In Chapter 4 – Results and Discussion, all relevant results are presented with a critical discussion. Finally, in Chapter 5 - Conclusions and Future Perspectives, the main conclusions are drawn, and future work is suggested to improve this project.

Chapter 2

LITERATURE REVIEW

2.1 Nanotechnology applied to health sciences

Nanotechnology is a field in frank expansion with promising results in diagnose and therapy procedures. Nanotechnology applied to medicine constitutes as open window to overcome the obstacles faced by classical methods. Namely, it allows a more sensitive and accurate detection of diseases, thus detecting them in early stages and allowing a premature start of treatments which may result in better prognosis [4, 5]. Nanotechnology implies the development and structural control of materials in a range of 1-100 nm. This small scale confers a very specific set of properties from bulk materials of the same composition [6]. The small size allows a very high surface-volume ratio and a higher reactivity of the materials due to higher exposition to the surface [1]. Currently, nanotechnology is being intensively explored in the development of different nanomedicines with very different applications. Many products based on nanotechnology have been approved by FDA for clinic use and others are in clinical trials stage (**Table 1** [6-8]).

3.2.1 Nanosystems for drug delivery

Nanotechnology is promising when applied to therapies and advantages of therapeutics using nano-based drug delivery systems have been extensively reported [9], namely in the encapsulation of bioactives [10]. Specifically, these systems allow improving the solubility of hydrophobic drugs, expanding the circulation half-life of the drug, specific targeting, circumventing immunogenicity and improving drug release profile [8]. NPs allow either a controlled release of encapsulated molecules over time or upon a specific stimulus (e.g. alteration of pH or temperature), which may reduce the frequency of administrations and increase the concentration in target tissues, resulting in less side effects [8]. NPs can be

functionalized and act on the activation/blocking of specific receptors, or act as carriers of multiple drugs simultaneously, making it an interesting tool for combined therapies [11]. Hence, nanotechnology confers great flexibility to the development of new formulations specifically designed for specific scenarios.

Essentially, nano-based drug delivery systems open an opportunity window for the therapeutic use of agents that cannot be used with conventional formulations due to low bioavailability or high instability [6]. The use of NPs as drug carriers can provide a safe and stable environment for the drug, and their properties may promotesiti a more efficient absorption of the encapsulated molecules. Hence, NPs are particularly interesting for orally delivered of biomolecules, as they can protect the drug against the harsh environment of gastrointestinal (GI) tract, improving their half-life [12].

Despite the potential of NPs to enhance drugs therapeutic effect has been proved through much research performed in the field for the past decades [13, 14], there is still a lack of scientific data and regulations regarding safe use of nano-systems in medicine. Therefore, pharmaceutical nanotechnology is still in infancy [15].

Currently approved nanosystems used for clinics are polymeric or non-polymeric [1] (**Table 1**). Regarding non-polymeric NPs, these can be metallic or liposomal. The first ones are not so commonly used but much progress has been done in their application for gene therapy and imaging techniques [16, 17], whereas liposomes are far more used. These systems can be composed of natural or synthetic amphiphilic molecules. Their physical and chemical properties are based on the net properties of the constituent lipids, including solubility, charge density and steric hindrance [18]. Due to the amphiphilic nature of these molecules, the formation of liposomes occurs spontaneously, in a self-assembly manner [19]. Liposomes are suitable for drug-delivery as they effectively protect encapsulated drugs from degradation, allow targeting to site of action and reduced toxicity. However, their applications are limited to some extent, owed to inherent problems such as low encapsulation efficiency, rapid release of hydrophilic drugs in the presence of blood components and short-term stability storage [14].

On the other hand, polymeric NPs offer some advantages over liposomes such as increased stability of the encapsulated drug and ease modification of NPs properties. For instance, size and surface characteristics can be easily manipulated and controlled drug release can be attained by adequate choice of matrix components [20].

Table 1 *– Nanosystems currently approved by FDA for clinical use and in clinical trials stage (adapted from [6-8]).*

Types of Nanosystems	Size (nm)	Characteristics	Applications	Examples
Carbon nanotubes	0.5-3 (diameter) 20-1000 (length)	High strength and unique electrical properties (conducting, semi-conducting or insulating)	Fluorescence bioimaging, multiphoton bioimaging, drug release, gene therapy, tissue engineering	
Dendrimer	<10	Highly branched and monodisperse polymeric systems	Controlled delivery of bioactives, MRI contrast agents	VivaGel (clinical trials)
Liposome	50-100	Phospholipid vesicles, biocompatible, versatile	Passive and active delivery of gene, protein, peptide and various other	Abelcet, DepoCyt, Myocet, Epaxal, Visudyne, AmBisome, DaunoXome,
Metallic nanoparticles	<100	Gold and silver colloids with high surface area to volume ratio, resulting in high area for functionalization	Magnetic-resonance imaging (MRI), magnetically guided drug delivery, magnetic biosensing and cell separation, gene therapy	Nanotherm, Feridex, GastroMARK (clinical trials)
Quantum Dots	2-9.5	Semi conducting material. Bright fluorescence, narrow emission, broad UV excitation and high photo stability	Fluorescence bioimaging, multiphoton bioimaging, fluorescence, in vitro diagnostics	
Polymeric Micelles	10-100	High drug entrapment, biostability	Long circulatory, target specif c active and passive drug delivery	Estrasorb
Polymeric Nanoparticles	10-1000	Biodegradable, biocompatible	Excellent carrier for controlled and sustained delivery of drugs. Stealth and surface modification nanoparticles	Copaxone, Genexol-PM, Adagen, Macugen, Pegasys, Neulasta, Somavert, Oncaspar, Renagel

2.2 Oral administration

Oral administration is the first option for drug delivery due to high patient compliance [21, 22] . However, it presents many hurdles, namely the low bioavailability of biomolecules and a delayed action when comparing to parenteral route of administration [23]. The low bioavailability of macromolecules administered through oral route is primarily related with large molecular size and solubility characteristics [24]. Namely, bioavailability has been reported to sharply decrease for molecules with a molecular mass higher than 500-700 Da, which is the case for most peptides and proteins [25]. Consequently, comparing to intra venous (i.v.) administration, to have the same bioavailability, a much higher dose of the drug is required. Also, for molecules to effectively be transcellularly adsorbed, a minimum of lipophilicity is necessary. Without this feature, adsorption can only take place by the paracellular pathway [10]. Nevertheless, most macromolecules used for therapeutic practices are hydrophilic, which poses a major obstacle for their oral absorption [26].

Despite this, due to high patient compliance, non-invasive character and lower risk of contaminations [27, 28], much research has been done to develop oral therapy alternatives to many different pathologies. The aim is to achieve the same benefits as the i.v. route while simultaneously avoiding the issues related to this administration method.

The main obstacle associated with the development of oral formulations is the high complexity of the GI tract which limits the absorption rate [21, 29]. Hence, NPs are particularly interesting for the orally delivery of biomolecules, due to the properties above mentioned.

One of the most successfully used polymers for drug delivery is poly (lactic-co-glycolic) acid (PLGA). PLGA is a synthetic, biocompatible and biodegradable polymer which has been widely used in the drug delivery field [30]. It degrades into monomeric metabolites of lactic acid and glycolic acid during its hydrolysis, that are easily metabolized via Krebs cycle [30-32]. PLGA allows a controlled release of the encapsulated molecule, through its slow degradation, thus prolonging therapeutic efficiency. Its safety profile has been assessed and PLGA is currently approved in various drug delivery systems, by both the US FDA and EMA, leaving PLGA-based NPs in a good position for clinical trials [30]. This polymer is commercially available with different molecular weights and copolymer ratios of lactic and glycolic acids which strongly affect its degradation time [33]. However, the most commonly used PLGA for NPs formulation is 50:50 PLGA.

When it comes to oral administration of NPs, toxicity can occur at a local level when NPs contact the GI tract cells or in a systemic manner, after and if the particles enter the blood

stream [34]. Therefore, the properties of the materials chosen to produce the NPs, surface architecture, charge and the size of the NPs play a crucial role in assuring successful results. All these variables can impact the success of these nanosystems by inducing alterations of the pharmacokinetic profile of the drug [31], and even the shape of the NPs may influence their interaction with the cells. The choice of the nature of NPs – polymeric or non-polymeric – as well as the polymers or proteins selected in their production and functionalization must be carefully done according to each specific application; all parameters must be adjusted to optimize the effects and reduce any possible side effects.

2.3 Gastrointestinal tract structure and composition

The GI tract is a hollow tube extended from the oral cavity to the rectum, comprising structures as the oesophagus, stomach, small intestine and the colon [28]. The movement of the muscles (peristalsis) along with the release of hormones and enzymes allow the digestion of ingested food as well as the processing of waste. Hence, the main function of the GI tract is the transport, digestion and selective absorption of nutrients, vitamins, minerals and electrolytes while simultaneously preventing the passage of pathogens, toxins and non-digested molecules [28].

To increase the absorption rate, the GI tract has a unique structure that is more evident in the small intestine where there are macroscopic valve-like folds, finger-like protrusion, cytoplasmatic extensions and crypts finger-like invaginations that strongly increase the exposed area of the epithelium (**Fig. 1**) [35]. The epithelium is composed by enterocytes which represent around 90% of all the intestinal cells and responsible for nutrient absorption. Goblet cells are dispersed in the intestinal epithelium and constitute up to 10% of this structure. Their main function is mucus secretion which aids on the expulsion of waste by lubricating the intestinal walls [29]. The mucus layer also acts as first defence mechanism by constraining most bacteria and preventing their penetration into the epithelium and also because it contains several different antimicrobial molecules as well as immunoglobulins [36, 37]. Apart from these there are small cell populations in the gut, namely Paneth which affect the innate immune system by regulating the gut microbiota. This is very important in the maintenance of the intestine homeostasis, as they contribute to a normal immune function [38]. Paneth cells also regulate

enteroendocrine cells that secrete several peptide hormones which are involved in regulating the physiological functioning of the gut.

Despite the selective absorption in the small intestine, and due to the high exposure of GI tract to pathogens, some of them manage to overcome the intestinal barriers inducing several diseases. For this reason, the intestine is the organ that possesses more lymphoid cells and produces more antibodies in the body than any other organ [28].

As the GI tract comprises different functions, along its length, several physiological parameters change depending on the main function of each specific region, increasing its structural and physicochemical complexity. These parameters include pH, superficial area, topology of the tissue, cell variety and gut microbiota and they must be taken in account in the design of a new oral therapeutic formulation as they constitute barriers to the action of the drug [28].

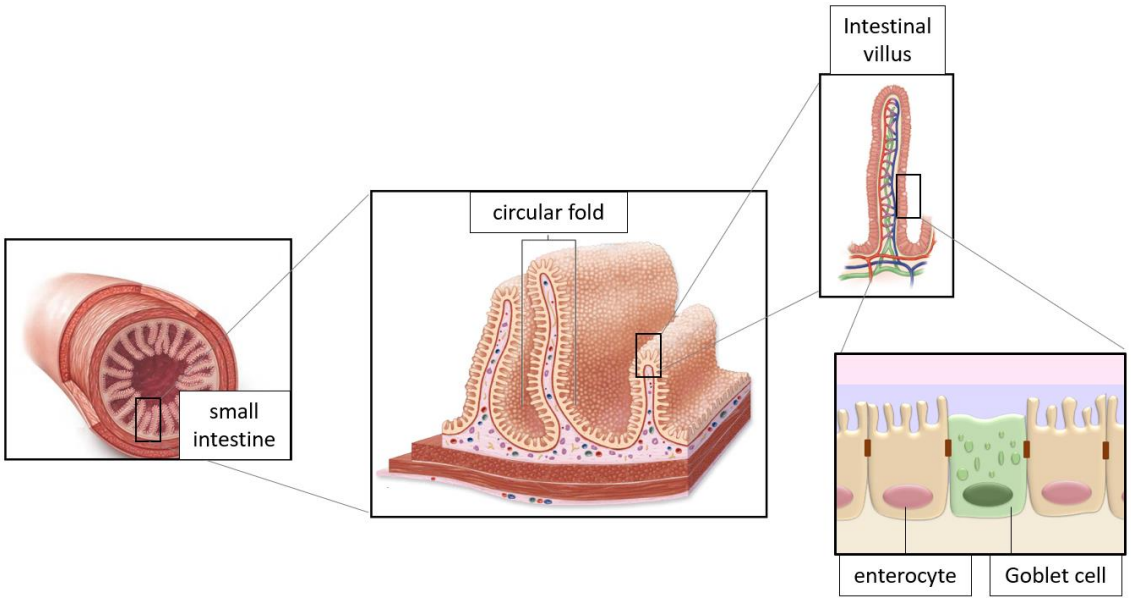

Fig. 1 – *Structure of the small intestine; cross section and small scale structures (adapted from [39-41]).*

2.4 Nanosystems as facilitators for crossing biological barriers

Recently, a few nanoparticle-based therapeutics have been approved for clinic use, to be administered through oral route [1]. NPs are particularly useful for the development of oral administration biomolecules as they can allow a higher success of drugs crossing the biological

barriers of the GI tract comparing to classical formulations. This is possible due to the stable and biocompatible environment they provide to the encapsulated drug, which may also be tuned to allow its controlled release rate and an efficient uptake by the epithelial cells of the intestine [42, 43]. Here, the residence time of formulations is very important to increase the absorption rate, particularly for systems that promote a slow releasing of the encapsulated drug [35].

To meet these criteria, formulations for oral delivery of biomolecules must be mucodiffusive and gastroresistant, allowing the structure integrity maintenance of the biomolecule and promoting a close contact to the intestinal epithelium where absorption occurs.

2.4.1 Gastroresistant structure

The low pH of the stomach milieu often induces the degradation of a very significative portion of the ingested drug [44]. To avoid this loss, the molecule of interest must be protected by a structure resistant to acidic conditions that undergoes degradation only in the intestine, promoting the drug release only at the absorption site [45]. This can be provided by embedding the NPs into an enteric matrix, i.e. in a matrix that is only soluble at pH equal or higher that the intestinal one (pH ≥ 6) or encapsulation in microparticles (MPs). Using a gastro-resistant structure would result in a controlled degradation of this compound, exposing the NPs to the lumen of small intestine.

Many enteric matrices have been described in the literature [46-48]. Among them, the polymer hydroxypropylmethyl cellulose acetate succinate (HPMC-AS) has been reported to act as gastroresistant matrix due to its pH dependent solubility [49] and has been already used in the development of sustained release formulations [49-51].

Different types of HPMC-AS which dissolve at different pH values, can be obtained by altering the ratios of acetyl and succinoyl groups (S/A) of the polymer. Type M (medium S/A ratio) would be more suitable for the application here suggested as the dissolution pH of the polymer is higher than 6 [50], which is the physiological pH of the small intestine [52].

2.4.2 Interaction with intestinal epithelium

The mucus layer in the epithelium is continuously renewed by Goblet cells and in association with peristaltic movements, it enables the excretion of digested products [28]. There

is a regulated balance between synthesis, degradation and removal of mucins, which defines the thickness of the mucus layer [53, 54]. In the small intestine, where absorption occurs, the thickness depends on the diet but overall it is less thicker than in the stomach or the colon to facilitate absorption [55]. The renewal rate of mucus is considerably high and greatly limits the drug residence time at the mucosa. The turnover time has been reported to vary from 50-270 min in rats [56]. Overall, the mucosal layer not only promotes a lower retention time of the NPs in gut but also prevents a close contact with the epithelial cells, thus affecting absorption [57].

For a more efficient mucosal drug delivery using NPs, two strategies are mainly utilized: (i) mucoadhesive and (ii) mucopenetration.

i) Poor permeability of proteins and peptides across biological membranes has been attributed to their hydrophilic structure and large molecular size. The interaction of these molecules with the mucosal layer strongly influences the success of the absorption in the intestinal epithelium [58]. Thus, the modification of drug carriers, such as NPs, with mucoadhesive polymers will allow a prolonged retention time. As mucus is essentially composed of 95% water and up to 5% glycoproteins (negatively charged), the polymers used for this approach should have positive charges [59]. The most commonly used for this purpose is chitosan (CS), a cationic polymer obtained from chitin deacetylation [60]. It is a biocompatible and biodegradable amino polysaccharide highly soluble in water at low pH [61]. It has been widely used in biomedical applications due to its low toxicity, antimicrobial and mucoadhesive properties [62]. Its mucoadhesive properties result from the interactions established with mucins, one of the main components of the mucus, but their nature is still poorly understood. However, previous studies have suggested that electrostatic interaction appears to play a crucial role in this interaction, followed by hydrogen bonds and hydrophobic effects [61]. Moreover, it has also been reported that LMW CS is able to increase drugs permeability by inducing a transient opening of cellular tight junctions [63-66]. Additionally, it can also help circumvent the immunogenicity induced by the formulation, as described in a previous study [67].

ii) On the other hand, mucopenetrating NPs can penetrate in deeper mucus regions to some extent, reaching even the epithelium of the absorption membrane [68]. Polyethylene glycol (PEG) has been extensively reported to reduce the interaction with mucus in the gut, when adequate molecular weight polymer is used [69]. Namely, PLGA NPs coated densely with low molecular weight PEG exhibited the highest mucus penetrating ability compared to loosely coated particles in fresh porcine intestinal mucus [70].

PEG is a hydrophilic and non-charged polymer commonly used in pharmaceutical applications [71]. Previous works have shown that thickly coated NPs diffuse through mucus

layers very rapidly as PEG effectively shields the interactions with the mucins, thus acting as mucopenetrant agent [43, 72-74].

Despite exhibiting different features, both mucoadhesive and mucopenetrating approaches have shown great potential for improved local and systemic therapeutic efficacy.

2.5 Nanoparticle-in-Microparticle systems

To conciliate both gastroresistant and mucodiffusing properties in a single system, one possible approach is the development of NiM structures, as depicted in **Fig.2**. As previously mentioned, the complex and highly variable structure of the GI tract hinders the absorption of biomolecules. To overcome the barriers to drug absorption, NPs encapsulating the biomolecule must be not only non-toxic but also interact in a close way with intestinal cells. The acidic gastric conditions induce not only the degradation of the encapsulated biomolecule with therapeutic effect but also the loss of conjugated biopolymers in the NPs surface, which justifies the need to encapsulate these NPs in a pH-responsive structure [75], as previously said in **section 2.4.1**.. An alternative to the development NiM systems, would be embedding of the NPs into a pH responsive capsule, designing the macrostructure of a tablet. However, the main problem of this approach is that, depending on the residence time in the stomach and the pH of the GI tract, may result in fast dissolution after exiting the stomach or it may pass the tract intact without any absorption occurring.

The major advantage of NiM systems is that these systems allow a controlled release of the encapsulated drug. Moreover, these systems allow not only multiple functionalities of the formulation but also the tuning of different features that can result in different releasing profiles, targeting and cellular interactions [76].

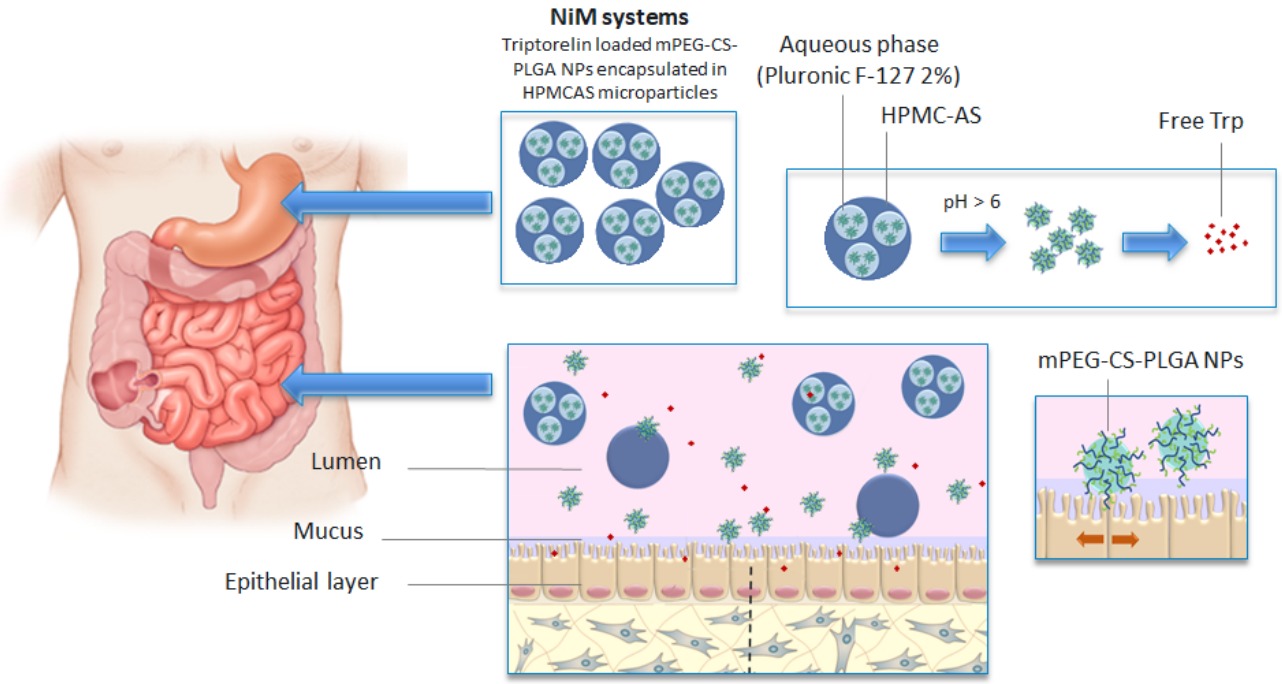

Fig. 2 – Representation of the mucoadhesive and gastroresistant nanoparticle-in-microparticle systems developed for triptorelin encapsulation.

2.5.1 Microfluidics for microparticles production

Research with MPs started in the early seventies and since then, many different polymers have been used in their production [77]. However, currently there are still very few microparticle drug delivery formulations approved for clinical use [78]. Like NPS, these systems can be prepared by several different methods, such as single or double emulsion, nanoprecipitation, by adjustment of the parameters that allow size control of the final formulation. Though, these conventional bulk approaches, do not allow a precise control of properties, namely because the mechanisms responsible for mixing of the different phases are stirring, shaking or homogenization, which result in different ratios between phases and low reproducibility [79]. This has led to an emergence of microfluidic platforms that help overcoming this hurdle by providing much more uniform formulations. The high reproducibility of batch-to-batch attained using microfluidics, namely regarding particle average size, distribution and surface charge, make it a promising approach for the development of novel therapeutics [80, 81]. Moreover, this methodology allows the production of drug carriers in a more time and cost-efficient manner.

2.6 Encapsulated drug: Triptorelin

In this work we will use a Trp as model peptide to develop the NiM system. There are numerous proteins and peptides with clinic application with limited biovailability when administered through the oral route, thus, the successful development of this NiM system could potentially be translated to other biomolecules encapsulation.

Trp is a synthetic decapeptide which is an analogue of Gonadotropin-releasing hormone (GnRH), currently used in clinic, in the form of acetate or pamoate salts [82], as a therapy for prostate cancer, endometriosis and breast cancer and in assisted reproductive techniques (ART). This molecule was developed to interact with the GnRH receptor and alter the release gonadotropins follicle stimulating hormone (FSH) and luteinizing hormone (LH) thus controlling the release of sexual hormones (**Fig.3**). Higher doses are used for metastatic prostate cancers whereas the lowest ones are used for assisted reproduction techniques. It is currently administered through intramuscular or subcutaneous injection, with a monthly dose of 3.75 mg, 11.25mg if administered every trimester or 22.5 mg for administration every six months [82, 83].

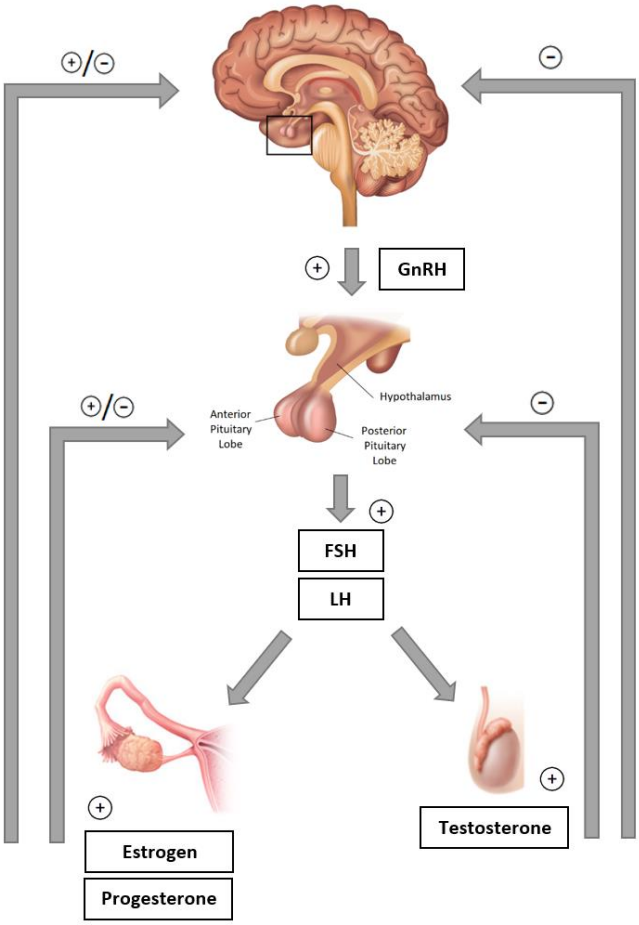

Fig.3 – *Triptorelin mechanism of action.*

In physiological conditions, there is a pulsatile release of GnRH by the hypothalamus promoting an intermittent stimulation of the pituitary gland [84]. A permanent stimulation of the hypothesis can be achieved by continued administration of the analogue Trp. This permanent stimulation induces the downregulation of its activity by negative feedback. Thus, besides having a longer action than natural GnRH, Trp also has a biphasic effect which GnRH does not; after an acute or intermittent administration there is a sudden increase of FSH and LH levels but upon continued treatment, these hormone levels decrease due to desensitization of the GnRH receptor, resulting in a profound decrease in plasma levels of LH, FSH, oestrogen and testosterone [82, 85].

Chapter 3

MATERIALS AND METHODS

3.1 Materials

PLGA-COOH (Purasorb PDLG 5004A; 50:50 lactide:glycolide molar ratio) and hydroxypropylmethyl cellulose acetate succinate (HPMC-AS) (AQOAT) enteric polymer were kindly provided by Corbion (Amsterdam, The Netherlands) and by Shin Etsu, respectively. Ethyl acetate was purchased from VWR® and N-(3-Dimethylaminopropyl)-N'-ethylcarbodiimide hydrochloride (EDC), 2-(N-morpholino)ethanesulfonic acid (MES) hydrate > 99.5% (tritration), mPEG (MW:5kDa) and Pluronic F-127 (hydrolyze grade > 80%) were purchased from Sigma-Aldrich®. The CS used has low molecular weight and was kindly provided by Kitozyme, and trehalose hydrate > 99.0% was purchased from Fluka Analytical.

For *in vitro* studies the cell lines used were C2BBe1 Caco-2 clone and HT29MTX cell lines that were obtained from American Type Culture Collection (ATCC, USA) and kindly provided by Dr.T.Lesuffleur (INSERMU178, Villejuif, France), respectively. Cells were cultured in Dulbecco's Modified Eagle Medium from Gibco™ supplemented with 5% (v/v) essential aminoacids, 5% (v/v) penyncilin-streptomycin and 10% (v/v) of inactivated foetal bovine serum. Permeability assays were performed using Millicell® Cell Culture (1.0 µm PET) in 6-well plates.

3.2 Methods

3.2.1 PLGA nanoparticles production

PLGA nanoparticles were produced by double emulsion. Briefly, 100 mg of the polymer was dissolved in 1 mL of EA overnight. For loaded nanoparticles 5mg of Trp acetate were dissolved in 100 µL of an aqueous solution, or for bare nanoparticles, ultrapure water was added alone. The solution was homogenized for 30 sec at 70% amplitude using VibraCell Model: VC50, from Sonics & Materials. After, the suspension was inverted into 4 mL of the Pluronic F-127 (2% v/v) solution and sonicated once again in the same conditions. Finally, the solution was inverted into 7.5 mL of Pluronic F-127 (2% v/v) and left for 3h under stirring to induce organic solvent

evaporation. The formulations were stored a 4°C and subsequently concentrated and washed. Using Amicon Ultra-15 Centrifugal Filter Units (Millipore) with a molecular weight cut-off (MWCO) of 100 kDa, the samples were added 10 mL of ultrapure water and centrifuged three times at 550 × *g* for 25 min (Eppendorf 5810R Refrigerated Centrifuge) or until concentration of volume to 1.5 mL. Samples volume was adjusted to 2 mL using ultrapure water and stored at 4°C.

3.2.2 Carbodiimide chemistry

The PLGA nanoparticles were conjugated with PEGylated chitosan to increase their interaction with the intestinal mucosa, thus enhancing the exposure of the nanoparticles to the epithelium [86]. This functionalization is more effective if done through chemical bonding instead of adsorption as it is possible that adsorbed polymers detach during nanoparticles washing steps. The COOH terminal group of PLGA will allow conjugation with PEGylated-chitosan through carbodiimide chemistry. In order to do so, a previous carbodiimide conjugation was performed to obtain mPEG-CS. Chemical conjugation of mPEG-CS and mPEG-CS-PLGA is represented in **Fig.4**.

3.2.2.1 Chitosan conjugation with polyethylene glycol (carbodiimide conjugation chemistry)

For this project, the conjugation of mPEG-CS is intended to have a substitution degree of around 10% as it is necessary that some amines remain free in the final structure, to interact with the negative charges of the mucins in the intestinal mucus. Each mole of PEG has one free carboxylic group to interact with the free amines of the CS. CS is a polymer constituted by randomly dispersed units of glucosamine and N-acetyl glucosamine, with many free amines to conjugate through carbodiimide coupling chemistry. This chemistry works by activating the carboxyl groups from PEG for direct reaction with free amines of the CS via amide bond. The stoichiometry of the conjugation was adjusted, and it was used a molar ratio of CS(NH_2):mPEG of 10:1.

Briefly, CS was dissolved in 1% (v/v) acetic acid solution overnight and pH was adjusted to 5 to allow complete dissolution. mPEG-COOH (Mw: 5kDa) at 1:10 molar ratio to CS was added

to the previous solution, with NHS (1:1 molar ratio to CS) and left understirring. EDC was added (1:1 molar ratio) gradually and solution was left at RT under stirring overnight. The solution was then concentrated and washed thrice using ultrapure water through AF (YM30, cut-off of 10kDa), in cycles of 1h, at 1800 × *g*. Final solution was freeze-dried to recover CS-mPEG in a white foam form.

3.2.2.2 Methoxypoly(ethylene glycol)-chitosan conjugation with PLGA NPs

Conjugation of mPEG-CS to PLGA NPs was performed through a second carbodiimide reaction. The ratio of PLGA:mPEG-CS used was 1:1 (w/w) and 10:1, 10:10 and 10:100 (molar ration) and the reaction was performed in MES (pH=5.5). EDC and NHS were added in a 1:1 molar ratio to PLGA carboxylic groups. The solution was left under stirring ON, protected from light. As control, same protocol was performed in the absence of EDC and NHS, to assess adsorption of mPEG-CS to PLGA NPs. Afterwards, different washing methods for the formulations were used. One method used was washing through AF with miliQ water, or with 0.1% acetic acid solution using AF before washing with miliQ water, to assess the relevance of the adsorption process in the carbodiimide conjugation. Dyalisis was also performed using a 100 kDa membrane cut off, as this method is less aggressive and less prone to induce aggregation or mass loss.

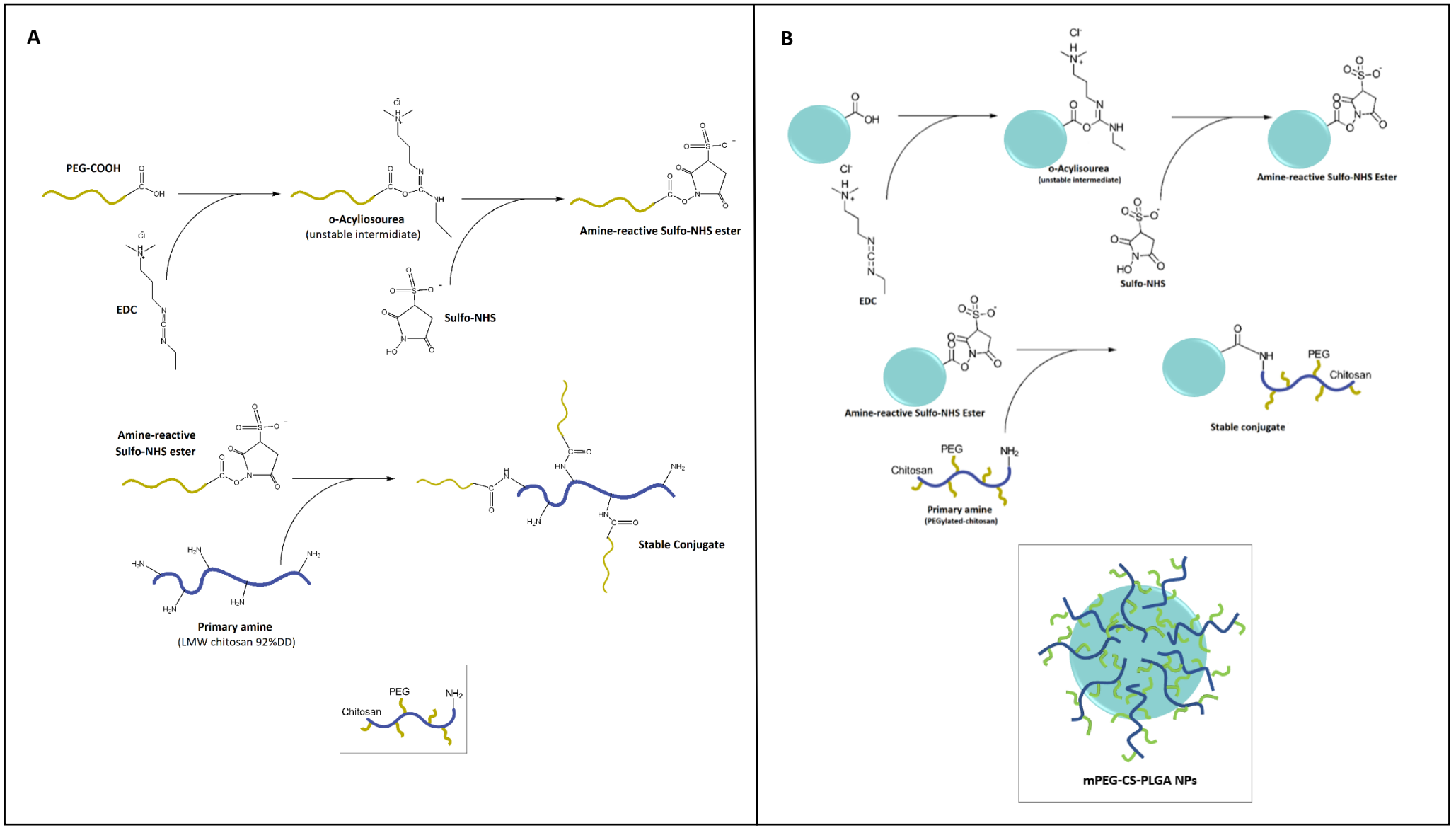

Fig. 4 – *Conjugation through carbodiimide chemistry of (A) mPEG with chitosan, and (B) of PLGA NPs with mPEG-CS.*

3.2.3 *Fourier-Transform Infrared Spectroscopy analysis of methoxypoly(ethylene glycol)-chitosan conjugate*

ATR-FTIR spectra of each sample were generated by ABB MB3000 FTIR spectrometer from ASEA Brown Boveri (ABB Zurich, Switzerland) equipped with a MIRacle single reflection attenuated total reflectance (ATR) accessory from PIKE Technologies (Madison, WI, USA). All spectra were collected with 256 scans and a 4 cm^{-1} resolution in the region of 4000–600 cm^{-1}.

3.2.4 *Nuclear Magnetic Resonance analysis of methoxypoly(ethylene glycol)-chitosan conjugate and conjugated nanoparticles.*

Proton Nuclear Magnetic Resonance (^{1}H NMR) analysis was performed, using an Avance III spectrometer from Bruker operating at 400 MHz (9.4 Tesla), to evaluate the efficiency of conjugation of mPEG-CS and of mPEG-CS-PLGA. Briefly, 12 mg of lyophilized sample were dissolved in 600 µL of adequate deuterated solvent, D_2O for mPEG-CS conjugate and DMSO-D6 for mPEG-CS-PLGA NPs. Analyses were performed at RT and chemical shift values were expressed in δ (ppm).

3.2.5 *Dynamic Light Scattering analysis of nanoparticles*

Characterization of NPs was also performed through DLS using 10 µL of the formulation diluted in 1 mL of 10 mM NaCl (pH=7.3). Average Z-size, PdI and ζ-potential were assessed using a DLS cuvette DTS1070.

3.2.6 *Nanoparticle Tracking Analysis*

NPs formulations were resuspended in ultrapure water, with a dilution factor of 1.0×10^5 for PLGA NPs and 1.0×10^4 for mPEG-CS conjugated or adsorbed PLGA NPs.

3.2.7 *Storage and freeze-drying*

For freeze-drying process, mPEG-CS conjugate was stored at -80°c overnight in open falcons covered with perforated parafilm. Then, all samples were left to freeze-dry at -80°C in vacuum conditions for 48 h.

Same procedure was used for lyophilization of conjugated and adsorbed NPs in a solution of 1% (m/v) trehalose and which has been reported to induce optimal reconstruction of NPs formulations [87]. This cryoprotective agent is a very versatile agent that helps preventing NPs collapsing after freeze drying process [88] and suitable for NPs encapsulating peptides.

3.2.8 *Drug Loading and Association Efficiency quantification by indirect method*

DL and AE was assessed through indirect method, using HPLC. A calibration curve was attained for different concentrations of the free Trp (2, 5, 12.5, 25, 50, 75 and 100 µg/mL) and used to estimate the amount present on the supernatant of the loaded NPs formulation (theoretical loading of 0.5, 0.75, 1 and 5% of Trp).

HPLC assay was performed according to the protocol provided by Ferring Pharmaceuticals in three different days to allow more accurate results. Briefly, an isocratic method was used, with a mobile phase comprised of tetrahydrofuran (THF) (21%) and 0.2 M triethylammonium phosphate (TEAP) (79%). Detection was performed by UV at 210 nm wavelength and the column used was C18 reverse phase which was kept at 50°. Each run lasted 10 min with peaks occurring at 7 min.

After integration of the peaks, AE and DL were calculated by the following equations.

$$AE\ (\%) = \frac{Inital\ mass\ of\ Trp - Total\ Trp\ mass\ in\ supernatant}{Initial\ mass\ Trp} \times 100 \quad (1.1)$$

$$DL\ (\%) = \frac{Inital\ mass\ of\ Trp - Total\ Trp\ mass\ in\ supernatant}{Total\ mass\ of\ the\ formulation} \times 100 \quad (1.2)$$

3.2.9 *Transmission Electron Microscopy*

The morphological features of NPs were analyzed by transmission electron microscopy (TEM) with a JEOL JEM 1400 (JEOL Ltd.) microscope at an accelerating voltage of 120 kV. Images were digitally recorded using a Gatan SC 1100 ORIUS CCD camera (Warrendale). Samples were prepared by dropping 10 µL of NPs formulations in a 1:20 dilution onto a 300-mesh nickel grid. All samples were stained with uranyl acetate.

3.2.10 *Metabolic Activity assays*

To assess possible cytotoxicity induced by mPEG-CS PLGA and by Trp loaded NPs in i*n vitro* models, a MTT assay was performed. Caco-2 clone and HT29MTX cell lines were seeded in a density of 0.2×10^6 per well with 200 µL of complete DMEM (10% FBS, 1% non-essential aminoacids and 1% Pen-Strep), in 96 well plates with 5 replicates per condition. The cells were incubated at 37°C, 5% CO_2 and washed once with PBS 1× 24h after. The conditions tested were free Trp, Trp loaded PLGA NPs, empty PLGA NPs, mPEG-CS, mPEG-CS-PLGA (conjugated through carbodiimide coupling chemistry) and mPEG-CS-PLGA (by adsorption). The concentrations for NPs formulations herein used were normalized in the results to the drug loading (DL) of the NPs; 2.59×10^{-2}, 2.59×10^{-1}, 2.59, 2.59×10^{1} and 2.59×10^{2} µg/mL. For Trp, the concentrations ranged from 0.1 to 1×10^{3} µg/mL in a logarithmic scale. Positive and negative controls were cells in complete culture medium and in triton X-100 (2%), respectively.

After incubation period, cells were washed with PBS 1X once again and incubated for 4h with MTT (0.5 mg/mL) reagent in the dark. After discarding the solution, DMSO was added to each well and incubated for 20 minutes in the dark in an orbital shaker (100 rpm). To calculate cell viability, absorbance was measured for 590nm and 630 using a Synergy Mx microplate reader (BioTek, Winooski, VT, USA).

3.2.11 *Permeability assays*

3.2.11.1 *In vitro culture*

The techniques employed to obtain the models used for the in vitro experiments were described in Araújo et al. [89]. Briefly, the Caco-2 clone and Caco-2 clone/HT29-MTX cocultures

were seeded on the apical chamber of 6-well Transwell plates in a density of 1×10^5 cells/cm^2 in each insert. For co-culture the proportion of Caco-2 clone to HT29-MTX used was 90:10 to mimic the physiological abundance of these cells in the intestine milieu. All conditions depicted in **Fig.5**.

3.2.11.2 Cell Monolayer Integrity

The TEER of mono-cultures and co-cultures was measured every time that the medium was replaced to check the confluence evolution and their integrity during the 21 days before the permeability studies. Moreover, the TEER values were measured before and after the transport experiments to ensure the integrity of the monolayer.

3.2.11.3 Permeability Studies

Before starting permeability assays, the culture medium was removed, and the cell monolayers were washed. HBSS was used to wash the cells before transport experiments and to prepare the suspensions to be tested in all the in vitro experiments developed in this work (monoculture and coculture). The basolateral chamber was filled with 2.5 mL of HBSS and the apical chamber was filled with 1.5 mL of drug formulation. The permeability studies were carried out from apical-to-basolateral direction in an orbital shaker at 37 °C and 100 rpm. After removing the cell culture medium, the Transwells were washed twice with prewarmed fresh HBSS buffer and equilibrated for 30 min. Then, 1.5 mL of nanoparticles corresponding to an amount of 100 µg/mL of Trp were pipetted into the apical side of the inserts. At different time points (15, 30, 60, 120 and 240 min), 200 µL of samples were taken from the basolateral side of the inserts and replaced the same volume of prewarmed fresh HBSS. The integrity of the cell monolayers was checked before and after the permeability experiments by measuring the TEER using Millicell-Electrical Resistance System (Millipore, USA). The quantification of the drug was performed by HPLC, following the same method used for DL and AE determination.

The percentage of permeability was calculated considering a continuous change of the donor and receiver concentrations, and it is valid in either sink or non-sink conditions [90].

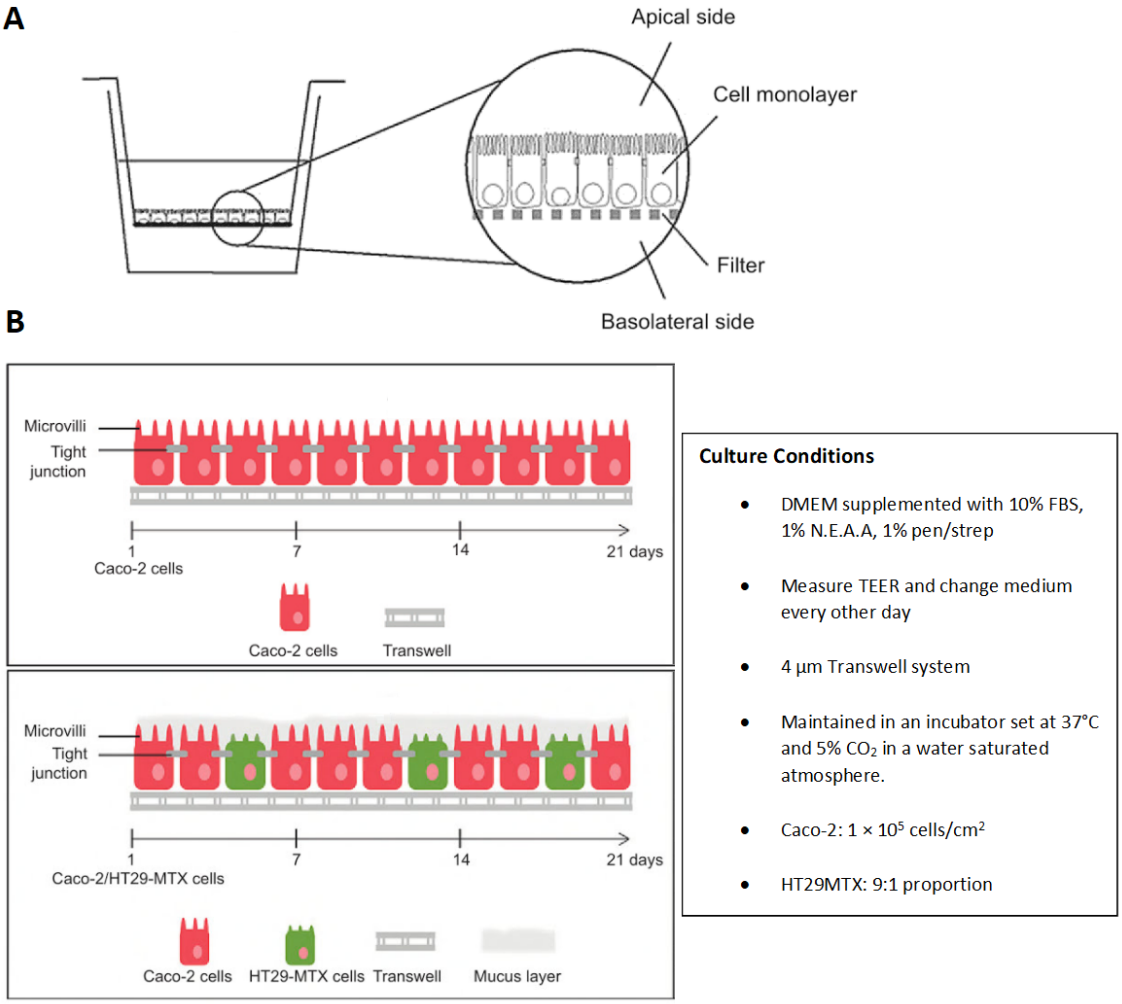

Fig. 5 *– (A) Schematic representation of a Transwell system. Reprinted from [91]. (B) Illustration of Caco-2 monoculture and Caco-2:HT29MTX co-culture model setup and culture conditions, reprinted from [92].*

3.2.12 Microparticle production

Nanoparticles (fresh and freeze-dried) were micro-encapsulated in an enteric polymer using a flow focusing geometry, through microfluidics. To prepare the Trp loaded NiM systems, 1 mL of Trp loaded NPs was added dropwise to 9 mL of 2% of HPMC-AS dissolved in ethyl acetate (organic phase). This solution was homogenized for 60 sec using a Vibra-Cell ultrasonic processor (Sonics, Sonics and Matrials, Inc., USA), originating to the first emulsion (w/o). This solution was then poured into a syringe to be injected in the microfluidic device as the inner fluid. The outer fluid used was an aqueous solution of 2% Pluronic F127 (water phase). The inner and outer fluids were both pumped into the microfluidic device in opposite directions at 50, 100 and 150 mL/h and 110, 210 and 430 mL/h, respectively.

This flow-focusing geometry used was assembled by gathering borosilicate glass capillaries on a glass slide, as described in [93].The chip consists in two types of capillaries, with the inner cylindrical tapered capillary fitting the inner dimensions of the square capillary, as presented in **Fig.6.** One terminal of the cylindrical capillary (World Precision Instruments, Inc.), presenting inner and outter diameters of 580 nm and 1000 µm, respectively, was tapered to 20 µm diameter, using a micropipette puller (P-97, Sutter Instrument Co.). Then, this diameter was increased to 80 µm using a microforge (P-97, Sutter Instrument Co.). The cylindrical capillary was placed into the square capillary, with and inner dimension 1000 µm (Vitrocom), and coaxially aligned. A transparent epoxy resin (5 minute ® Epoxi, Devcon) was used to fix the capillaries.

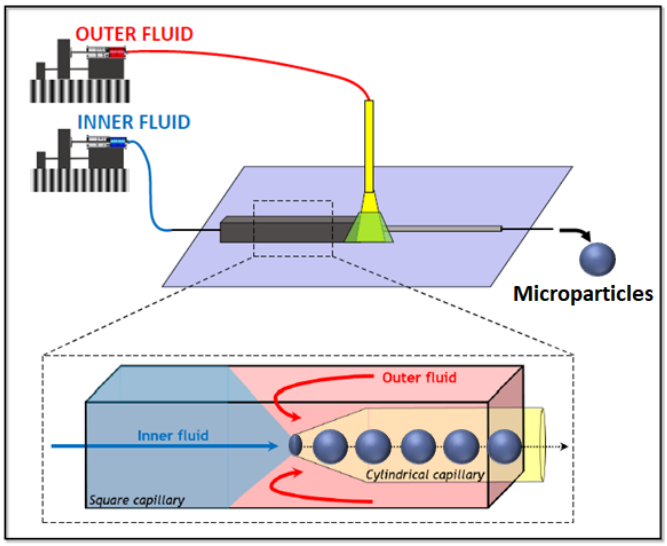

Fig. 6 *– Schematic representation of a setup used for production of pH responsive MPs through microfluidics. Reprinted from [94].*

This flow focusing geometry forces the inner fluid to breakdown, forming the second monodisperse emulsion (w/o/w) droplets at the entrance orifice of the tapered cylindrical glass capillary, as shown in Fig.6. The droplets were collected in a cylindrical beaker containing 15 mL of the aqueous phase, in order to facilitate the particles deposition. These particles were left 2h under stirring to evaporate the organic solvent. After recovery of MPs, these were washed by 5 min centrifugation cycles at 800 x g, in 10 mL of ultrapure water.

3.2.13 pH responsive degradation of microparticles

After collection and washing of the microparticles, these were incubated with different pH buffers. Briefly, 20 µL of sample were added in adequate SEM supports and the excess of water was removed with filter paper. Different buffer solutions at pH values of 1.2, 4, 5.5, 6.0 and 6.8, were added on top of the particles for 2 h. After 2 h, the excess of buffer solutions were removed with filter paper and the particles were allowed to dry at room temperature overnight.

3.2.14 Scanning Electron Microscopy analysis

For SEM analysis, the pellets of MPs obtained were resuspended in 1 mL of ultrapure water and then diluted in a 1:20 ratio**,** 2 µL of each sample was poured directly in an adequate support and left overnight to dry at room temperature.

For analysis of pH dependent degradation of microparticles, these samples were incubated with different pH buffers in suports with double sided carbon adhesive tape.

The SEM / EDS exam was performed using a High resolution (Schottky) Environmental Scanning Electron Microscope with X-Ray Microanalysis and Electron Backscattered Diffraction analysis: Quanta 400 FEG ESEM / EDAX Genesis X4M. Samples were coated with Au/Pd thin film, by sputtering, using the SPI Module Sputter Coater equipment, during 60 sec.

Chapter 4

RESULTS AND DISCUSSION

4.1 Nuclear Magnetic Resonance

Chitosan is a polymer obtained from deacetylation of chitin. Hence, in its structure there are acetylated and deacetylated monomers. The latter group correlates with the number of free amines in CS structure, and since CS may present different degrees of deacetylation (DD), this determination is necessary for calculation of the amount of PEG to use in chemical conjugation.

This value was determined by prior calculation of the degree of acetylation (DA) using the spectra presented in **Fig. 7**. DA was determined through integration of the NMR peaks of CS, using the equation reported in [95] at 3.8 ppm, that represents the protons depicted in the $C_{2\text{-}6}$ of the ring-skeleton of the same unit. These integrations were normalized to the peak occurring at 3.1 which represents H-2 proton of glucosamine residues, as depicted in **Fig. 7**. The DD of the CS used is 93%.

$$DA = [(1/3 \times I_{CH3})/(1/6 \times I_{(H2\text{-}H6)}) \times 100$$

$$DD = 100 - DA$$

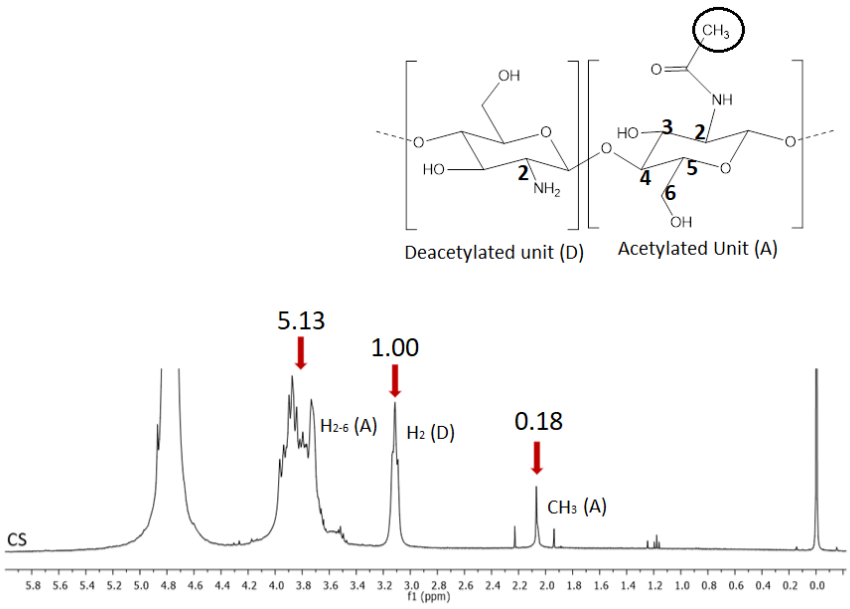

***Fig. 7** – NMR H^1 spectrum of CS.*

Chemically conjugation will be perfomed by carbodiimide chemistry, which creates amide bonds between the free amines of CS and the free carboxylic group of PEG.

Each mole of PEG has one free carboxylic group to interact with the free amines of the CS. As the conjugation was performed in a molar ratio of 1:10 of free carboxylic groups of the PEG to free amines of CS, the maximum theoretical substitution degree would be 10%.

The first carbodiimide conjugation (mPEG with CS) was assessed through NMR by integration and comparison of the peaks of mPEG-COOH, CS and the conjugate mPEG-CS (**Fig. 8**). The different samples resulting from conjugation reaction between mPEG and CS were dissolved in deuterated water (D_2O) and all mPEG-CS spectra were normalized and centred at 4.49 ppm, relative to the peak of that solvent [96]. This spectrum presented the peak related with the terminal methylene group unit of PEG (O-CH2-CH2-) depicted at 4.3 ppm and the H-2 proton of the acetylated unit of CS depicted at 3.2 ppm.

In addition, the appearance of the peak at 2.1 ppm attributed to the acetyl group (–COCH_3,), confirmed the presence of chitosan in the samples [97].

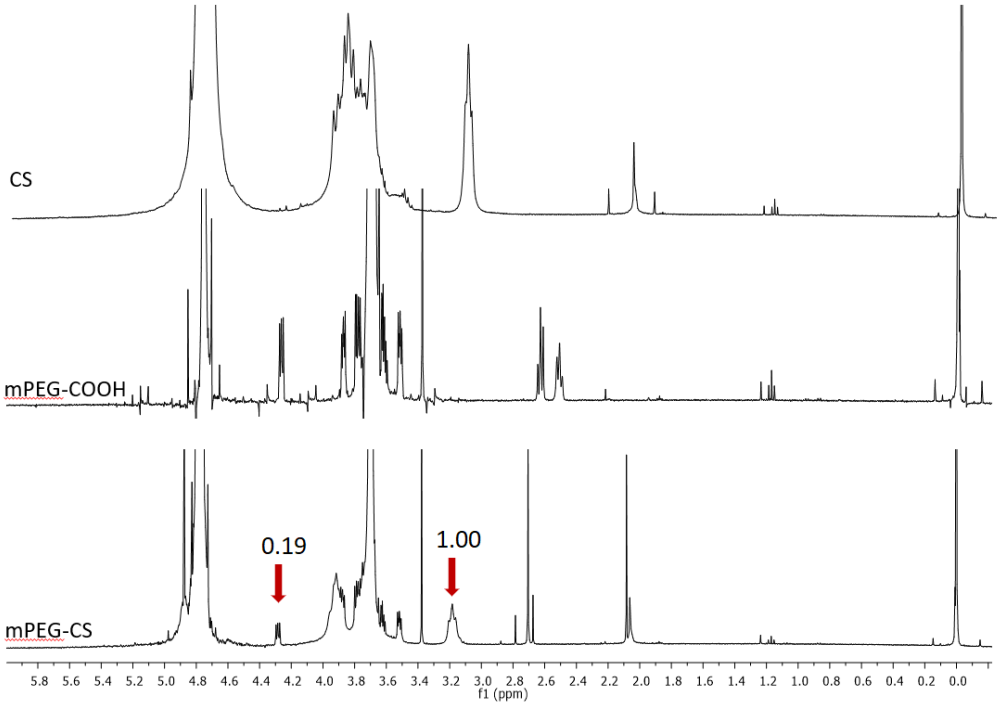

Fig. 8 *– H^1 NMR spectra of mPEG-CS conjugate.*

Using these two peaks, the substitution degree (SD) was calculated, by the following equation. Here, the integration of the aforementioned mPEG peak is 0.19, normalized to the CS peak.

$$SD = \frac{\frac{I_{PEG(-O-CH2-CH2-)}}{4}}{I_{CS(H-2)}} \times 100 \quad (1.3)$$

After calculation, the SD was of 4.75%, and this value was constant even when the experiment was performed several times, giving values within a range of 4.75% to 6.25%.

For the propose of the herein work, the conjugation should occur partially and not cover all free amines of CS structure, as it is necessary that some remain free to interact with the negative charges of the intestinal cells.

The PLGA-PEG-CS NMR spectra are presented in **Fig. 9** as well as the peaks relative with mPEG and CS already described above, and characteristic peaks of PLGA at 1.4 (3H), 4.8 (2H) and 5.2 (1H) ppm related to the -CH3, -CH2, and -CH protons of PLGA, respectively [98]. Furthermore, a broad peak was observed at 3.3 ppm, which is attributed to water [99].

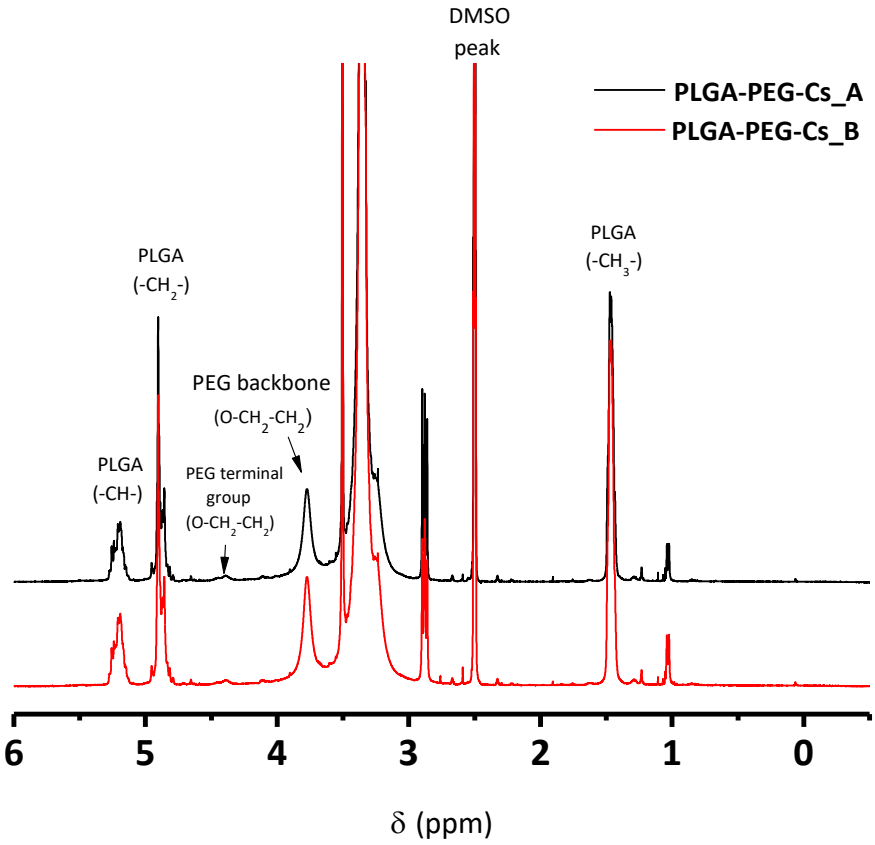

***Fig. 9** - H^1 NMR spectra of mPEG-CS-PLGA NPs.*

The PEGylation efficiency of PLGA was estimated by comparison between the PEG peak (3.7 ppm) and the integration of all PLGA peaks with a previously normalization to 4 and 6 peaks, respectively [98]. The results are presented in **Table 2**. Overall, the PEGylation efficiency of PLGA NPs was around 50 %.

Table 2 *– PEGylation efficiency.*

Sample	Peak intensity				PEGylation efficiency (%)
	3.8 (PEG)	1.4	4.8	5.2[a]	
PLGA-PEG-Cs_A	2.08	2.76	1.69	1	57.2
PLGA-PEG-Cs_B	1.90	2.89	1.75	1	50.5

[a]The peak at 5.2 ppm was set as 1.

4.2 Fourier-Transform Infrared Spectroscopy

Fourier-Transform Infrared Spectroscopy (FTIR) was also performed to corroborate this information. The IR spectra of CS has been described by Mi, Sung and Shyu [100, 101] with peaks occurring at 1660 cm^{-1} for -CO, at 1154 cm^{-1} for C-O-C and at 1598 cm^{-1} and 1651 cm^{-1} for -NH2, amide I and II, respectively. However, the obtained spectrum for mPEG-CS conjugate shown in **Fig.10**, presented no band for the amide bond, possibly due to the low detection limit of the technique.

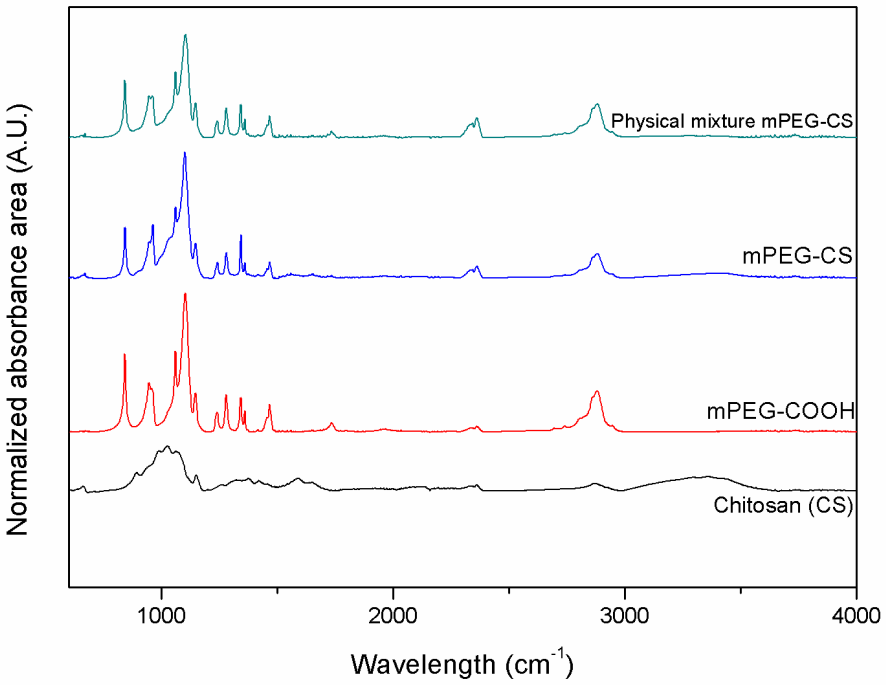

Fig.10 – *FTIR spectrum of mPEG-CS conjugate.*

The second conjugation (mPEG-CS with PLGA NPs) cannot be confirmed through this technique. Theoretically, FTIR identifies the amide bond that occurs between the carboxylic groups of PLGA and the amines of CS [102], which is already present in mPEG-CS conjugate, even though was not perceptible in the spectra shown. Consequently, the same spectrum would be obtained and the efficiency of the second carbodiimide conjugation could not be assessed. As an alternative, size and ζ-potential alterations were assessed through DLS, which can possibly lead us to the efficiency of the conjugation. The conjugation of the NPS with CS induces a slight increase in the size and decreases the negative charge of PLGA NPs, and has been already reported [62].

4.3 Characterization of Nanoparticles

PLGA NPs presented a size of around 200 nm and were monodisperse, as suggested by the low polydispersion index (PdI) (**Table 3**). As PLGA is a negatively charged polymer, the ζ-potential (ZP) of the NPs is also negative, as expected. PLGA NPs produced by nanoprecipitation

have been reported to have a ZP of -40 mV [103]. Here this value is less negative, possibly due to the use of Pluronic F-127 to stabilize the NPs. However, as the surfactant is not fully removed from the surface of the NPs in washing steps, an exposition of the carboxylic groups of PLGA that confer a negative charge to the particles maybe hampered.

Table 3 *– DLS results for formulations prepared with PVA or Pluronic F-127 as surfactants before washing.*

	Hydrodynamic size (nm)	PdI	ζ-Potential
PVA	198 ± 3	0.19 ± 0.01	-0.66 ± 0.04
Pluronic F-127	196 ± 9	0.18 ± 0.03	-1.93 ± 0.16

Hence, depending on the final application of these NPs, searching for efficient washing methods for these PLGA NPs could be essential. For instance, the presence of excess of surfactant may hinder the exposition of the carboxylic groups of PLGA in the NP surface, thus preventing an effective conjugation through carbodiimide chemistry. Through the methodology herein used, surfactants are strictly necessary to stabilize surface tension. To assess NPs washing method that had more consistent results for further analysis, two batches of PLGA NPs were produced using different surfactants, PVA and Pluronic-F127, both at 2% (v/v). Half of the volume of each formulation was used to perform washing through ultracentrifugation (UF) and the other half using Amicon Filters (AF) to evaluate which one resulted in better colloidal properties, with results presented in **Table 4**.

Table 4 *– DLS results for formulations prepared with PVA or Pluronic-F127 as surfactant and washed through ultracentrifugation or with Amicon filters (cut-off of 100kDa).*

		Hydrodynamic size (nm)	PdI	ζ-Potential
PVA	UC	245 ± 25	0.19 ± 0.03	-2.02 ± 0.37
	AF	194 ± 11	0.12 ± 0.01	-1.05 ± 0.15
Pluronic F-127	UC	336 ± 64	0.44 ± 0.05	-12.74 ± 1.77
	AF	176 ± 7	0.14 ± 0.02	-7.66 ± 0.36

PLGA NPs produced with Pluronic F-127 (2%) as surfactant and washed with the AF presented the best results, with sizes around 176 nm, a low PdI (0.14), demonstrating that these formulations were monodispersed, and charges of approximately -7.66 mV. Similar results were not observed for the same formulation when washed through ultracentrifugation as the pellet could not be resuspended even after sonication and the supernatant was not clear, indicating a

very polydisperse distribution of sizes. Both washing methods were not very successful at removing the surfactant from the NPs since the ZP comprised values of -7.66 ± 0.14 mV and -12.74 ± 1.77 mV, for the UF and AF respectively, which have been reported in the literature as expected results for non-washed particles [104]. This is due to the fact that pluronic is a neutral surfactant and thus its attachment on the surface of NPs decreases the negativity of their charge.

The formulations using PVA as surfactant were not suitable and both washing methods were even more ineffective in removing the surfactant from the NPs comparing to PLGA NPS with Pluronic F-127 (2%), as shown by the neutral charges presented for these formulations, which indicates a more extended cover of the PLGA NPs surface.

Considering the results obtained, the formulation that was selected for downstream analysis was the NPs produced using Pluronic F-127 (2%) as surfactant and washed with the AF.

Afterwards, the conjugation between the NPs and mPEG-CS was performed in a ratio of 1:1 (w/w). To assess the relevance of electrostatic interactions in the conjugation of mPEG-CS with PLGA, some of the formulations were washed in a 0.1% (v/v) acetic acid solution and characterized (data not shown). The rationale of this experiment was that this solution would induce a detachment of the mPEG-CS adsorbed to the surface of NPs, leaving only the chemically conjugated mPEG-CS to the PLGA. These results did not show any differences, possibly due to the cut-off of the filters used, which may have hampered the complete removal of the unbound mPEG-CS. Thus, even if the conjugate is indeed removed from PLGA NPs surface, it may interact again with the CS through electrostatic bonds. As the molar mass of CS was not provided by the supplier, the ideal cut-off the filters for washing the NPs is not known.

As observed in **Table 5**, both adsorption and chemical conjugation of mPEG-CS with PLGA NPs resulted in an increased size, compared to non-conjugated PLGA NPs. After washing NPs, both size and PdI slightly decreased which originated more uniform populations. In the conjugated formulations there were no observable aggregates immediately after conjugation. However, after the washing steps through AF, some aggregates were visible in both formulations. This compromised any downstream analysis as there was a visible loss of mass, which could not be identified as being PLGA or mPEG-CS in excess. The aggregation could have been caused by high speed in the centrifugation process or the very high volume used. There was a very significant loss of mass which hampers a correct determination of the concentration of the formulation. Thus, despite the consistent results of DLS, these formulations were not suitable for downstream analysis as a very considerable amount of mass was lost, and thus the theoretic concentrations had a big error associated with it.

Table 5 – *DLS analysis of PLGA NPs adsorbed or chemically conjugated with mPEG-CS in a 1:1 (w/w) ratio to PLGA before and after washing steps using AF.*

	Hydrodynamic size (nm)	PdI	ζ-Potential
PLGA NPs	183 ± 4	0.17 ± 0.02	-9.54 ± 0.56
mPEG-CS-PLGA NP (carbodiimide) (Before wash)	272 ± 6	0.34 ± 0.01	4.94 ± 0.13
mPEG-CS-PLGA NP (carbodiimide) (After wash)	222 ± 1	0.28 ± 0.03	7.63 ± 0.29
mPEG-CS-PLGA NP (adsorption) (Before wash)	292 ± 9	0.37 ± 0.33	5.05 ± 0.29
mPEG-CS-PLGA NP (adsorption) (After wash)	248 ± 2	0.34 ± 0.01	6.91 ± 0.60

The DLS equipment is based on light scattering, where the intensity fluctuations in the scattered light are analysed and related to the diffusion of the scattered particles. The results are strongly affected by the presence of large dimension contaminants, even when in small amount [105]. To confirm these results, besides DLS, also NTA was performed, but in this case, the formulation was diluted in miliQ water instead of 10 mM NaCl due to equipment requirements. NTA measures the particle size based on the observation of the trajectories of individual particle and their displacement by Brownian motion, by the equation of Stokes-Einstein. This system allows sizing particles from 30 nm to 1000 nm with the lower detection limit being dependent on the refractive index of the NPs [106]. The results of NTA measurement are presented in **Table 6** and it is possible to verify that when compared to DLS, all the formulations presented smaller sizes. The fact that the samples may not be perfectly monodisperse, can end in different results between these two techniques. Despite these values, the same trend is present with PLGA NPs being smaller than mPEG-CS conjugated PLGA NPs and as NPs will be further microencapsulated, a rigorous size distribution is desirable but not strictly necessary.

Table 6 – *NTA analysis of PLGA NPs adsorbed or chemically conjugated with mPEG-CS after washing steps using AF.*

	Dilution factor	Hydrodynamic size (nm)	Concentration (particles/mL)
PLGA NPs	1.0×10^5	128.2 ± 2.8 nm	$4.07 \times 10^8 \pm 1.53 \times 10^7$
PLGA:mPEG-CS NP (carbodiimide)	1.0×10^4	137.5 ± 5.0 nm	$3.32 \times 10^8 \pm 2.16 \times 10^6$
PLGA:mPEG-CS NP (adsorption)	1.0×10^4	139.9 ± 3.5 nm	$2.40 \times 10^8 \pm 8.43 \times 10^6$

NTA technique could be useful to assess the number of NPs in suspension and thus allow a more rigorous control of the conditions used in *in vitro* experiments. However, as DLS is the most well-established technique and the standard to assess hydrodynamic size and ζ-potential, it will be used instead of NTA in all characterization analysis.

Bearing in mind all the issues regarding the resuspension of the NPs from the AF, the conjugation with different molar ratios of mPEG-CS:PLGA were further tested (1:10, 10:10, 100:10). These ratios were calculated based on the number of free amine groups of CS and the carboxylic groups of PLGA. Here, the main goal was to attain good colloidal properties of the NPs; a monodisperse population and with a neutral or slightly positive charge. After conjugation and adsorption with the mPEG-CS, ZP should increase due to the positive charges of CS[62]. The results are presented in **Table 7.** It is possible to depicted that the changes in ZP were more significant in the NPs produced considering the 1:1 (w/w) ratio, where CS is present in excess. Nevertheless, this does not happen for the 1:10 and 10:10 molar ratio formulations. This suggests that CS was in low concentration and thus conjugation did not occur in great extent. For the first one, based on the size and ZP presented, it is suggested that not only no conjugation has occurred, but also there was a decrease of the ZP values, suggesting that the washing procedure further removed any surfactant remaining.

Considering this, the formulation selected for downstream studies was the 100:10 ratio, that will be referred onwards as 10:1. This formulation presented good results, with neutral values for ZP, indicating the presence of free amines as well as a narrow distribution of size range.

Table 7 *– DLS characterization of PLGA NPs and mPEG-CS-PLGA NPs adsorbed or chemically conjugated.*

		Hydrodynamic size (nm)	PdI	ζ-Potential
PLGA NPs		182 ± 4	0.17 ± 0.02	-9.5 ± 0.6
PLGA:mPEG-CS NPs (adsorption) (1:1 (w/w)		248 ± 2	0.34 ± 0.01	6.9 ± 0.6
PLGA:mPEG-CS NPs (carbodiimide)	1:1 (w/w)	222 ± 1	0.28 ± 0.03	7.6 ± 0.3
	1:10	184 ± 12	0.20 ± 0.03	-16.9 ± 1.0
	10:10	438 ± 128	0.44 ± 0.04	-8.9 ± 0.6
	100:10	287 ± 33	0.36 ± 0.05	-0.2 ± 4.0

4.4 Transmission Electron Microscopy

As observed through TEM, all formulations present a spherical shape with size average around 200 nm, which has been reported for PLGA-CS NPs [107].

The main goal here was to corroborate the DLS results as well as to visualize the shape of the NPs and the absence of aggregates. Nevertheless, the images depicted in **Fig.11** suggest that there is more than one sized population for all formulations, as the sizes are not even, with some NPs presenting a size of a few dozen nm.

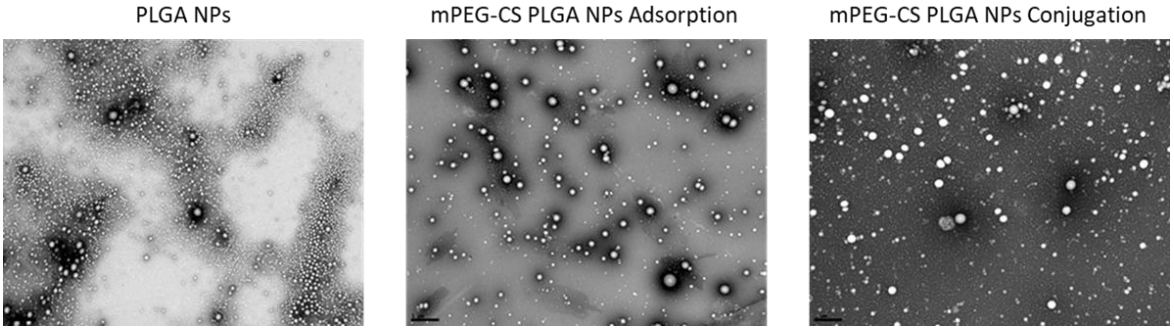

Fig. 11 *– TEM analysis of PLGA NPs and adsorbed and chemically conjugated mPEG-CS-PLGA NPs. Magnification 12000X.*

4.5 Determination of Drug Loading

The AE and DL of Trp was determined through High Performance Liquid Chromatography (HPLC), according to the protocol provided by Ferring Pharmaceuticals. An isocratic method was used, with a mobile phase comprised of tetrahydrofuran (THF) (21%) and 0.2 M triethylammonium phosphate (TEAP) (79%). After preparation of loaded NPs, the samples were washed through AF and the supernatants were recovered. These supernatants were then quantified by HPLC and the AE and DL were calculated based on the amount of Trp present on the supernatant of the NPs. The method herein used is an indirect method for the assessment of AE and DL as it did not imply the destruction of NPs for quantification of the drug.

Using the mobile phase mentioned, we obtained short and wide peaks as presented in **Fig. 12**, which were not suitable for attainment of calibration curve, as the lower concentrations of the peptide might not be detectable. Due to the equipment limitations, the method had to be performed at RT and it may explain the delay of the retention time of triptorelin observed.

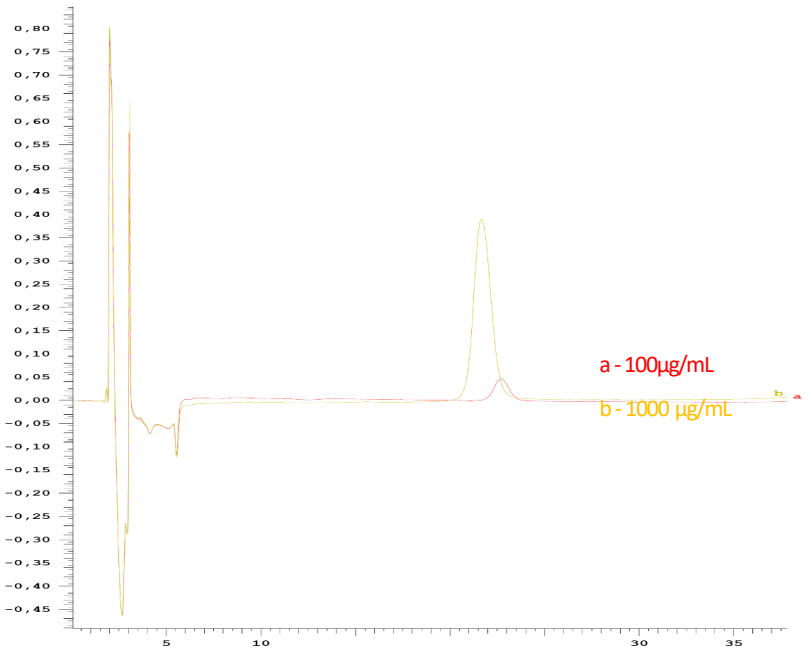

***Fig.12** – HPLC peaks obtained for free Trp (100 µg/mL and 1000 µg/mL) with column at RT.*

These results suggest that to obtain the calibration curve, the method needs optimization as the peaks should occur earlier and must be more evident. Column and samples temperature, as well as the concentration of the mobile phase, are variables that can be adjusted for better results.

The temperature variable was addressed, and the assay was performed with the column at 50°C. Samples were prepared in triplicates at a concentration of 5 µg/mL, 12.5 µg/mL, 25 µg/mL, 50 µg/mL, 75 µg/mL and 100 µg/mL, with peaks occurring at 7min.

As good linearity was attained as shown in **Fig.13**, loaded NPs could be produced and the AE and DL can be assessed through the indirect method. To assure no significant differences were observed between empty and loaded NPS, DLS characterization was performed to batches of 500 µg, 750 µg, 1000 µg and 5000 µg of Trp loaded NPs.

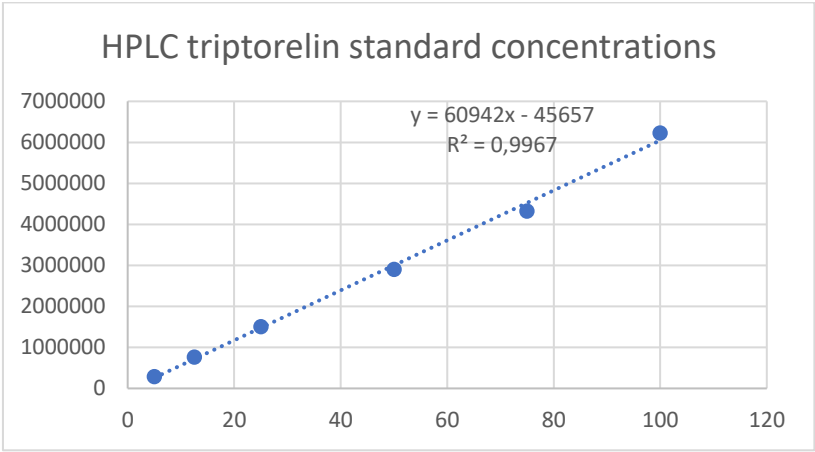

Fig. 13 *– Linear regression attained using the areas of the peaks obtained for of 5 µg/mL, 12.5 µg/mL, 25 µg/mL, 50 µg/mL, 75 µg/mL and 100 µg/mL of free Trp.*

As observed in **Table 8**, the batches prepared for a theoretical DL of 5% were the ones presenting better results regarding AE and DL without significant differences in size or ZP with the other formulations. Thus, this was the selected formulation for posterior *in vitro* analysis. Nevertheless, these values are calculated not having in consideration the possible losses that occurred during conjugation with mPEG-CS. This happens because NPs undergo dialysis after conjugation, to remove any remaining reagents in solution, and due to the big volume used, Trp is very diluted and cannot be detected through HPLC.

Table 8 *– DLS characterization of Trp loaded NPs.*

		Hydrodynamic size (nm)	PdI	ζ-Potential	AE (%)	DL (%)
Trp	500 µg	185 ± 5	0.19 ± 0.01	-7.9 ± 0.1	39	0.20
	750 µg	178 ± 6	0.16 ± 0.02	-8.2 ± 0.0	38	0.28
	1000 µg	179 ± 4	0.16 ± 0.01	-7.3 ± 0.1	42	0.42
	5000 µg	182 ± 2	0.16 ± 0.01	-7.7 ± 0.2	54	2.59

4.6 Metabolic Activity Assay

To assess any possible cytotoxic effects induced by mPEG-CS-PLGA formulations and the drug, Caco-2 and HT29-MTX cell lines were seeded and incubated with all formulations and positive and negative controls during 4 h and 24 h. 4 h time-point was selected due to posterior *in vitro* analysis of formulations. More specifically, this was the highest time point selected for permeability studies and this experiment was to assure that no toxicity was observable throughout this period. Thus, the formulations would not induce any disruption on the cell monolayers during permeation studies. 24 h time-point was selected to ensure that even if the formulation is in contact with the intestinal epithelial for a long time, namely in the event of chronic administration, minimal toxicity would occur.

Regarding the concentrations selected for NPs, these were calculated based on the DL efficiency calculated and normalized to the amount of peptide per 100 mg of PLGA for all formulations. As mentioned before, this drug is administered through parenteral routes with highest doses being administered in a 6-month basis, of 22.5 mg. Testing concentrations as high as 259 µg/mL of Trp, which are way over the real amount currently administered, we can state that if proven safe, any concentration below this limit will be non-cytotoxic too.

All formulations had been previously freeze-dried and were resuspended in complete medium before being added to the cells. As no cryopreservant was used at this stage, most formulations showed some aggregation. This might be due to the fact that PLGA is highly hydrophobic and removing the water during the freeze-drying process results in a closer contact between particles, promoting stronger interactions between them. As an attempt to mitigate this hurdle, all formulations were homogenised for 30 sec and vortexed prior to incubation with cells.

The results presented in both **Fig. 14** and **Fig. 15** show that there is no tendency of increased toxicity with increased concentrations, but this might be related to the variability issues aforementioned. Nevertheless, one can observe that after incubation of 4 h in both cell lines, the metabolic activity is higher than 70%, suggesting no cytotoxic potential [108], apart for the highest concentration tested of free Trp in Caco-2 culture, and PLGA NPs in HT29-MTX culture.

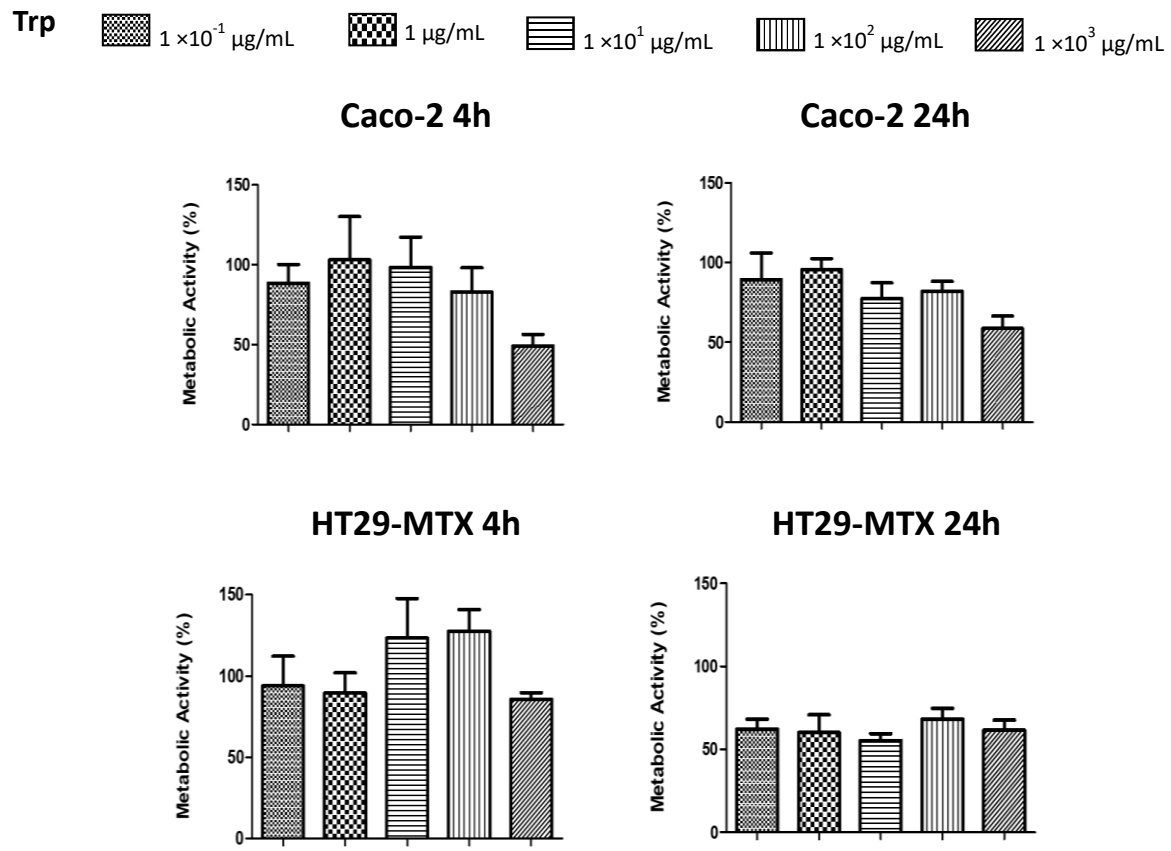

Fig. 14 *– Metabolic activity of Caco-2 and HT29-MTX cell lines after incubation with free Trp for 4h and 24h.*

For 24 h incubation, metabolic activity decreases comparing to 4 h incubation. For Caco-2, only PLGA NPs at 2.59 µg/mL and 2.59 × 10^2 µg/mL concentration, and free Trp at 1 × 10^4 µg/mL result in a metabolic activity under 70%. For HT29-MTX, there are more formulations decreasing cells metabolism under this value, being that particularly significant for Trp loaded NPs. Also, for longer incubation times, it is worth noticing that even when the metabolic activity

is higher than 70% [108], it is closer to this limit, suggesting an overall higher toxicity with incubation times.

In HT29-MTX cells, for both 4 h and 24 h incubation, mPEG-CS-PLGA NPs both adsorbed and chemically conjugated, present the highest metabolic activity for all concentrations, suggesting a safest system than the PLGA NPs alone. However, this does not happen for Caco-2 cells, with similar metabolic activity occurring in the presence of conjugated and non-conjugated NPs.

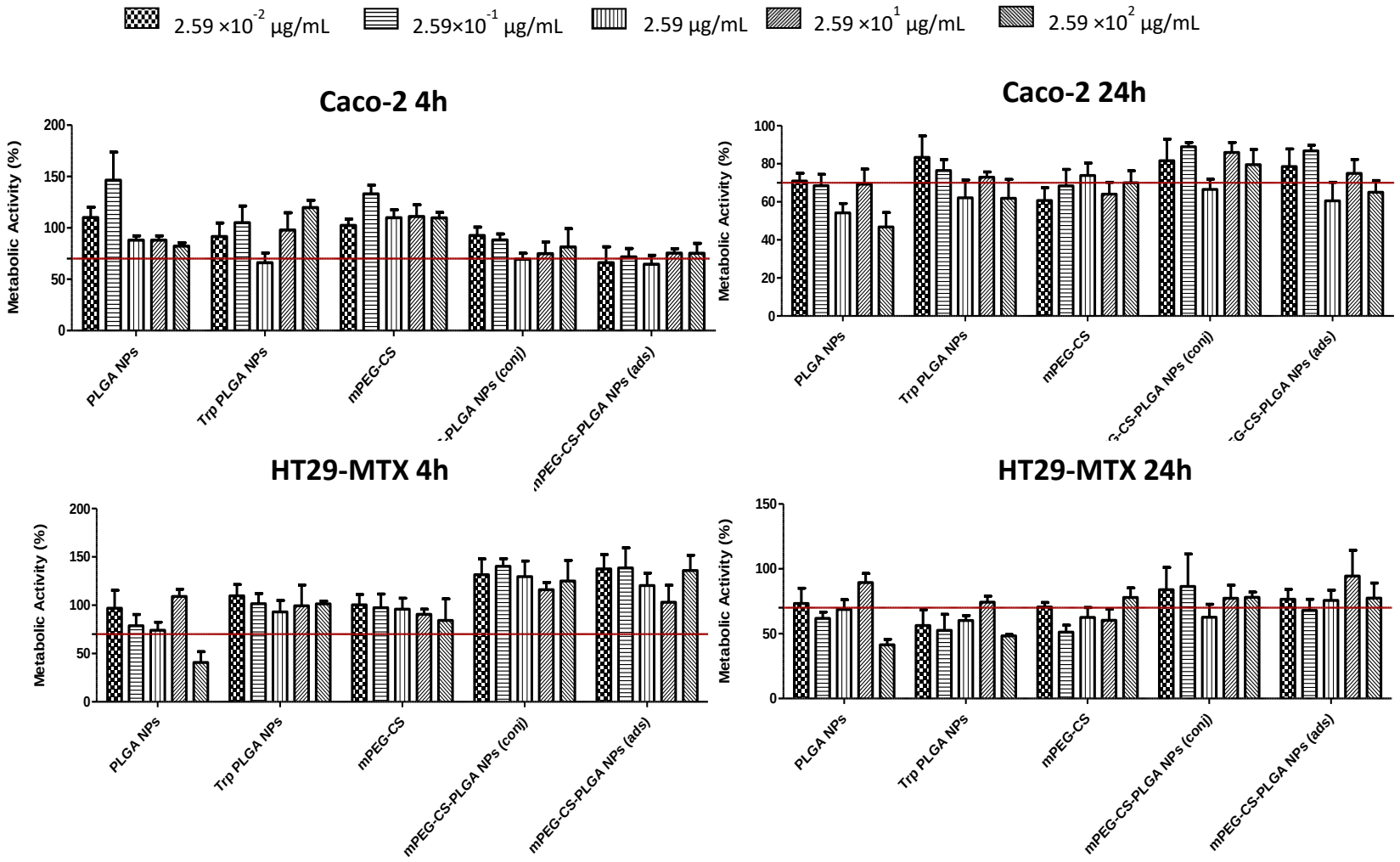

Fig. 15 – *Metabolic Activity of Caco-2 and HT29-MTX cell lines after incubation with NPs formulations for 4 h and 24 h (n=4).*

4.7 Permeability Assays

To assess whether NPs formulations have any effect over the permeability of Trp in the intestinal epithelium, permeability assays were performed in Caco-2 monoculture and Caco-2:HT29MTX co-culture models.

Due to the abundance of tight junctions in differentiated Caco-2 monolayers, this model has been reported to have higher TEER values when compared to co-culture [109]. Namely, TEER values for a well-established monolayer in Caco-2 cell line, have been reported to vary between 150 to 1000 $\Omega.cm^2$, decreasing with higher passage numbers [110, 111]. Values below this limit are usually indicators of leaky monolayers. However, is important to stress that physiological TEER values are much lower than the ones presented *in vitro* by Caco-2. Human intestinal epithelium presents TEER values that range from 20 $\Omega.cm^2$ in the jejunum to 100 $\Omega.cm^2$ in the large intestine [110]. This may be pointed as one limitation of this model to mimic the intestinal epithelium. One other limitation is the fact of not including goblet cells, the second most prevalent population in the intestinal epithelium, hence the need for establishing a co-culture model.

HT29-MTX cells are derived from human intestinal goblet cells, which comparing to absorptive Caco-2 cells, have a lower expression of tight junctions. This has been reported to correlate with an increased paracellular permeability to hydrophilic compounds of Caco-2 co-cultured with HT29MTX, compared to Caco-2 alone [112].

In the herein study, 21 days prior to permeability assay, cells were incubated with supplemented medium, which was changed every other day, coinciding with TEER recordings to assess the integrity of the monolayer over time. Results are presented in **Fig.16.** The monoculture was expected to have higher TEER values compared to the co-culture, which was not observable. Nevertheless, the values of both models were kept constant during the assay, suggesting that the cell monolayer did not suffer any alterations during the experiment (**Fig. 17**).

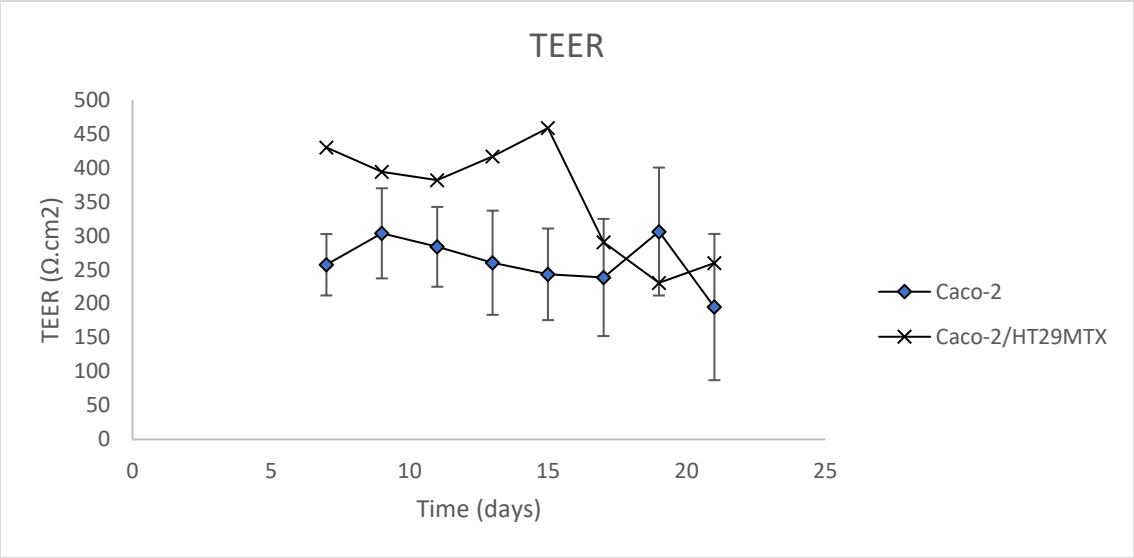

Fig. 16 *– TEER values of Caco-2 monoculture and Caco-2/HT29MTX Co-culture.i*

Permeability results, presented in **Fig.17**, suggest that the conjugation with mPEG-CS seems to have no significant effect on facilitating Trp permeation through the cell models. One can speculate that this is due to the release profiles of Trp when encapsulated, since PLGA has a slow release kinetics. Therefore, the release is not fast enough and there is no big amount of Trp in the medium to be permeated. To access the release profile of the drug is a main priority in future studies. Moreover, other layers conferred by the mPEG-CS may also hindered the release of the peptide. Nevertheless, no conclusions can be drawn regarding this, due to the uncertainty of the presence of an intact monolayer prior to the permeability assays, mainly in the Caco-2 monolayer, as the TEER values are close to the limit of minimum acceptable for a sturdy monolayer. Another factor that limits any illation is the high standard deviation present in most samples. This occurred due the fact that quantification of Trp by HPLC for NPs formulations and mainly for the first time-points, resulted in very low quantities of drug permeation, which occurred in the limit of linearity of the curve established for standard concentrations of the free peptide. The peaks occurring were very small and often hard to integrate from the background, resulting in very high variability between identical samples.

As observed in **Fig. 17**, free Trp is able to cross the cell monolayers at a higher rate when compared with the NPs formulations, being that trend expected and consistent since the first time-points. The drug permeability is higher for the co-cultured, despite not statistically significant, compared to the monoculture which is consistent with the lower expression of tight junctions and thus a facilitated paracellular permeation of hydrophilic compounds.

Regarding non-conjugated NPs, in the Caco-2 model, it seems to allow a faster release of the encapsulated drug compared to the NPs with modified surface (**Fig.17**). This may be related to the absence of other layers conferred by the mPEG-CS modification. Without mPEG-CS, PLGA is more exposed to the cellular milieu and may experience a faster degradation, resulting in a higher release of the encapsulated drug. On the other hand, mPEG-CS-PLGA NPs may present an additional barrier to the degradation of the NPs, and thus result in a very slow release of Trp. For the co-culture model, same tendency of the monoculture was observed but without statically significant differences between drug permeability for NPs formulations.

CS has been long known for its mucoadhesive properties, being currently used in the modification of liposomes and NPs to improve the drug delivery through mucosal surfaces [68]. Additionally, LMW CS has also been described to induce transient tight junctions opening, thus facilitating the paracellular passage of drugs [42]. Hence, it was expected that a slight decrease of TEER values occur for both mono and co-culture during the permeability experiment, which was not observable.

Overall, permeability of Trp was too low, and formulation needs optimizations. Nonetheless it is important to stress that this study was performed in buffer solution, with no enzymes present and thus it is likely that PLGA degradation occurs at a much slower rate than it would in the physiological milieu.

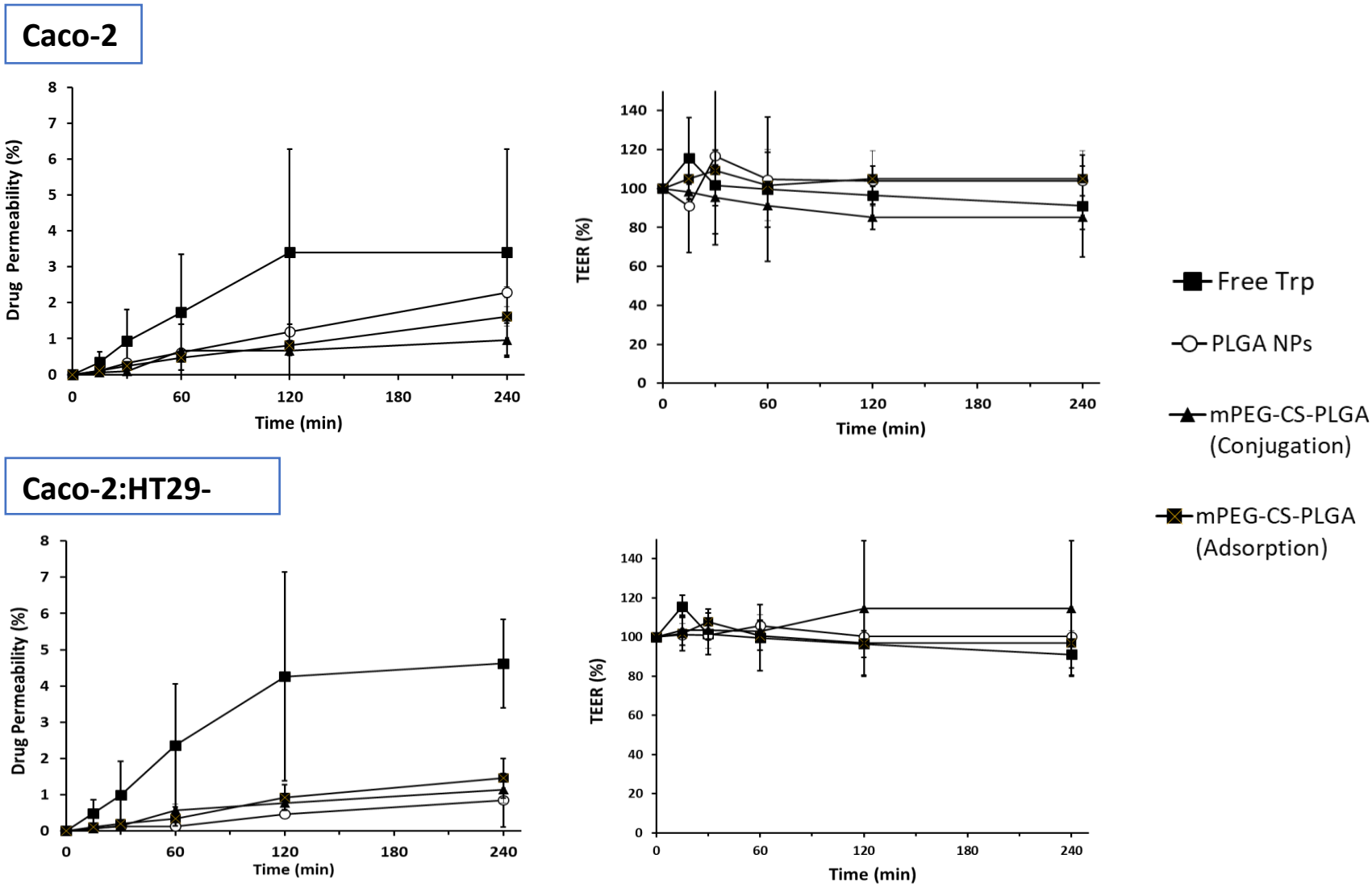

Fig. 17 *– Evaluation of Trp permeation in Caco-2 and Caco-2/HT29MTX models with monitorization of TEER values for all time-points.*

4.8 Scanning Electron Microscopy

Considering the results of the freeze-drying process and all the issues regarding their resuspension afterwards, new batches were produced adding 1% (m/v) of trehalose to the suspensions after dialysis, for SEM analysis. Concentrations of 1-10% of trehalose have been reported to induce optimal reconstruction of PLGA NPs [87], and the lowest concentration was used to minimize microencapsulation of high amounts of sugar in the next stages of this work.

As an attempt to remove this step to the process, PLGA NPs were chemically conjugated in a smaller volume of MES buffer, (1mL per 10mg of PLGA instead of 1mL per 1mg of PLGA) allowing a higher concentration of the final formulation, eliminating thus the freeze drying. These formulations were analysed through DLS and presented similar results to the ones conjugated in higher volumes (data not shown).

Both fresh and freeze-dried formulations were used to produce MPs using a flow-focusing geometry depicted in **Fig. 18**, and observed through SEM to assess morphology and size distribution (**Fig.19 and Table 9**). Here we tested different flow rates for the organic phase, keeping the aqueous phase constant at 430 mL/h. The main goal here was to observe if this parameter would induce significative size alterations in the MPs.

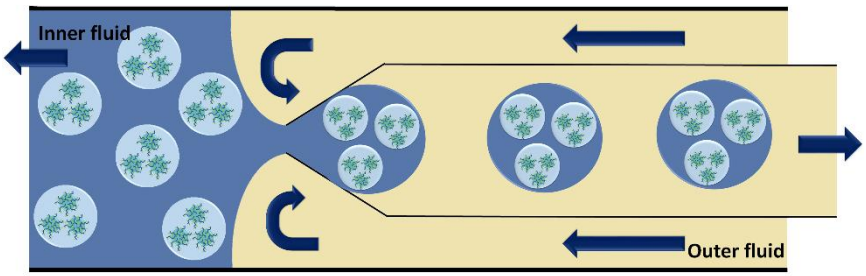

Fig. 18 – *Schematic representation of a flow focusing device used for production of pH responsive MPs through microfluidics (adapted from Araújo et al, 2015 [89]).*

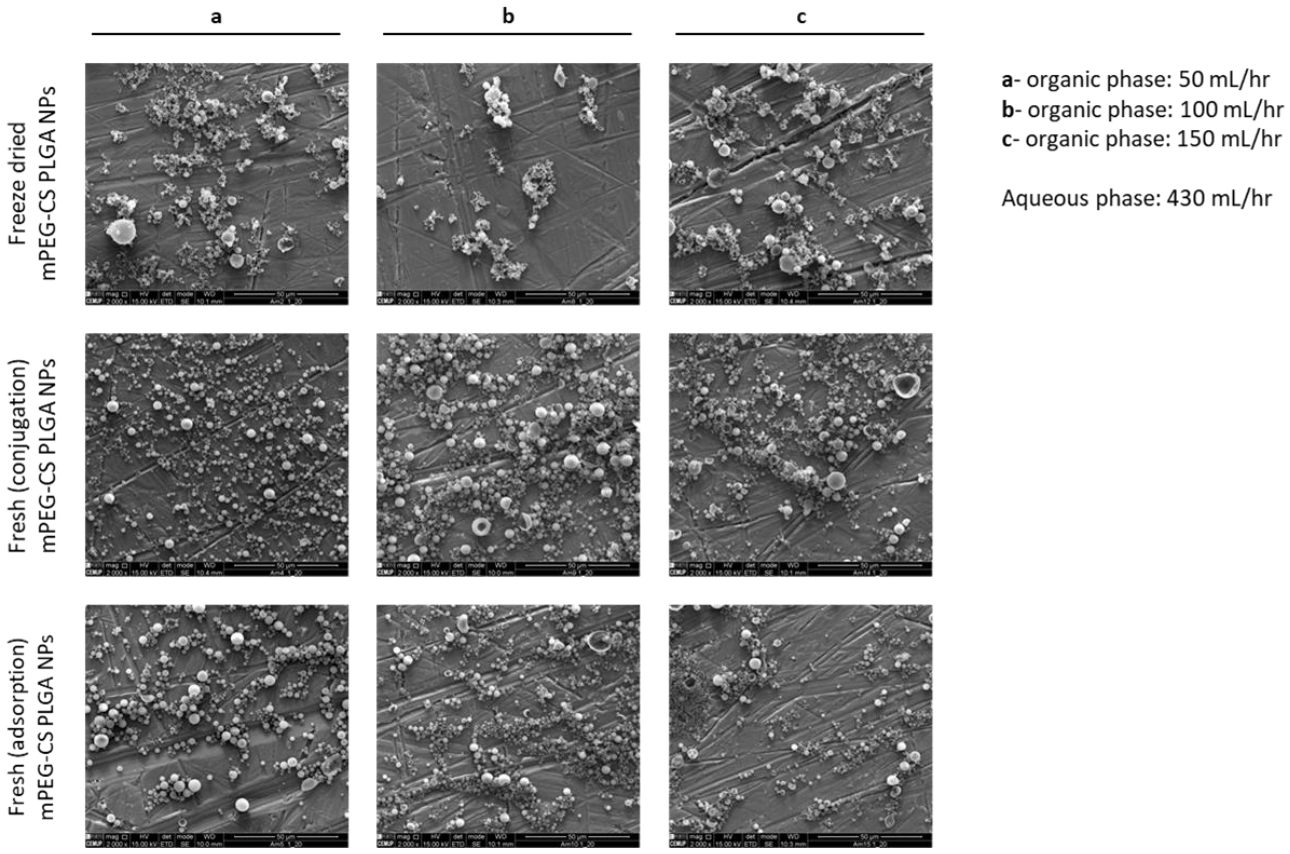

Fig. 19 – *SEM images of MPs.*

Regarding the freeze-dried formulations, several aggregates of particles were observable, which were probably the conjugated NPs, and not the MPs, as the first ones presented a similar size range after the freeze drying process and hence could not be successfully encapsulated. On the other hand, the MPs obtained for fresh conjugated NPs were not aggregated. Since the size of these NPs previously to the microencapsulation was around 200 nm, which are not seen in the images, it is possible that either the PLGA NPs are sensitive to electrons rays, vacuum conditions or the coating process itself and collapsed or degraded. Or else, it is possible that they were indeed encapsulated in these systems and thus cannot be identified alone.

Regarding the influence of the flow speed in size distribution, there were not any significant differences. Nevertheless, with higher flows for the organic phase, there was a higher occurrence of particles collapse, and thus, 50 mL/hr appears to be the most adequate flow for further NiM systems.

Table 9 *– Average size of the MPs produced using different flow rates of the organic phase, with aqueous phase kept constant at 430mL/h.*

	Size (µm)		
	FD mPEG-CS-PLGA NPs	mPEG-CS-PLGA NPs (ads)	mPEG-CS-PLGA NPs (carb)
50 mL/h	2.43 ± 2.25	2.29 ± 1.19	2.82 ± 1.75
100 mL/h	2.33 ± 1.41	2.75 ± 1.83	2.15 ± 1,09
150 mL/h	2.68 ± 1.47	2.62 ± 1.64	2.11 ± 1.23

To try and address the hypothesis raised regarding the NPs being or not encapsulated into the MPs, an elementary analysis was performed, on the surface of the sample. PLGA NPs were conjugated with mPEG-CS, which contains nitrogen atoms on the deacetylated unit of CS. Since this compound is not present in the HPMC polymer used for MPs production, the detection of nitrogen would indicate that the particles present are not the MPs, but the mPEG-CS-PLGA particles instead.

As shown in **Fig. 20**, and as expected, the main elements detected were C and O, highly present in PLGA, mPEG and HPMC. Au and Pd are also present in the coating and Al from the surface of the support was also detected. The absence of N may be due to its presence in a quantity below the detection limit or due to the fact that NPs were indeed encapsulated and thus there is no N in the surface of the HPMC MPs.

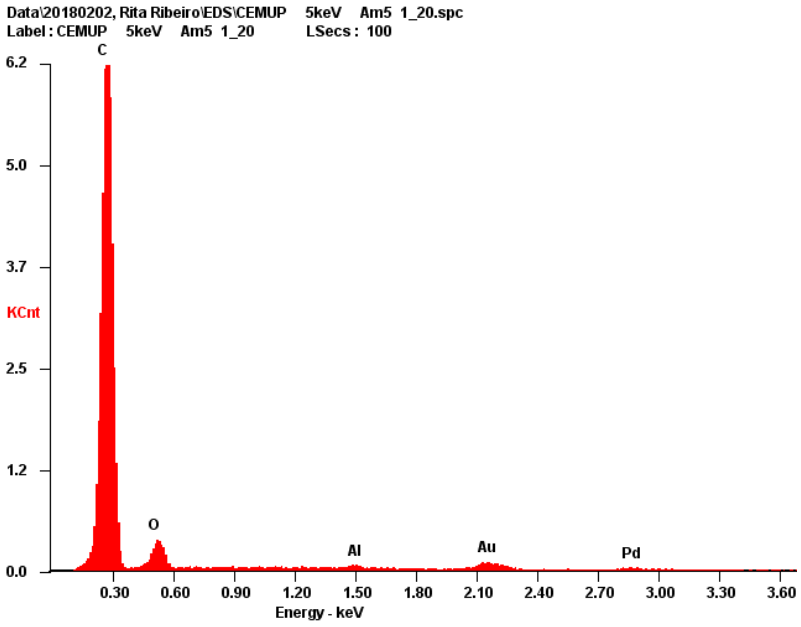

Fig. 20 *– EDS spectra of microencapsulated mPEG-CS-PLGA NPs for elementary analysis.*

The size of the MPs could be increased to allow encapsulation of more NPs per particle, thus further optimization of flow rates can be done. Since 50 mL/h of organic phase presented good results regarding MPs integrity, this parameter will be kept constant and the flow rate of the aqueous phase will be decreased. The flow rates tested for the aqueous phase were of 110 mL/h and 210 mL/h.

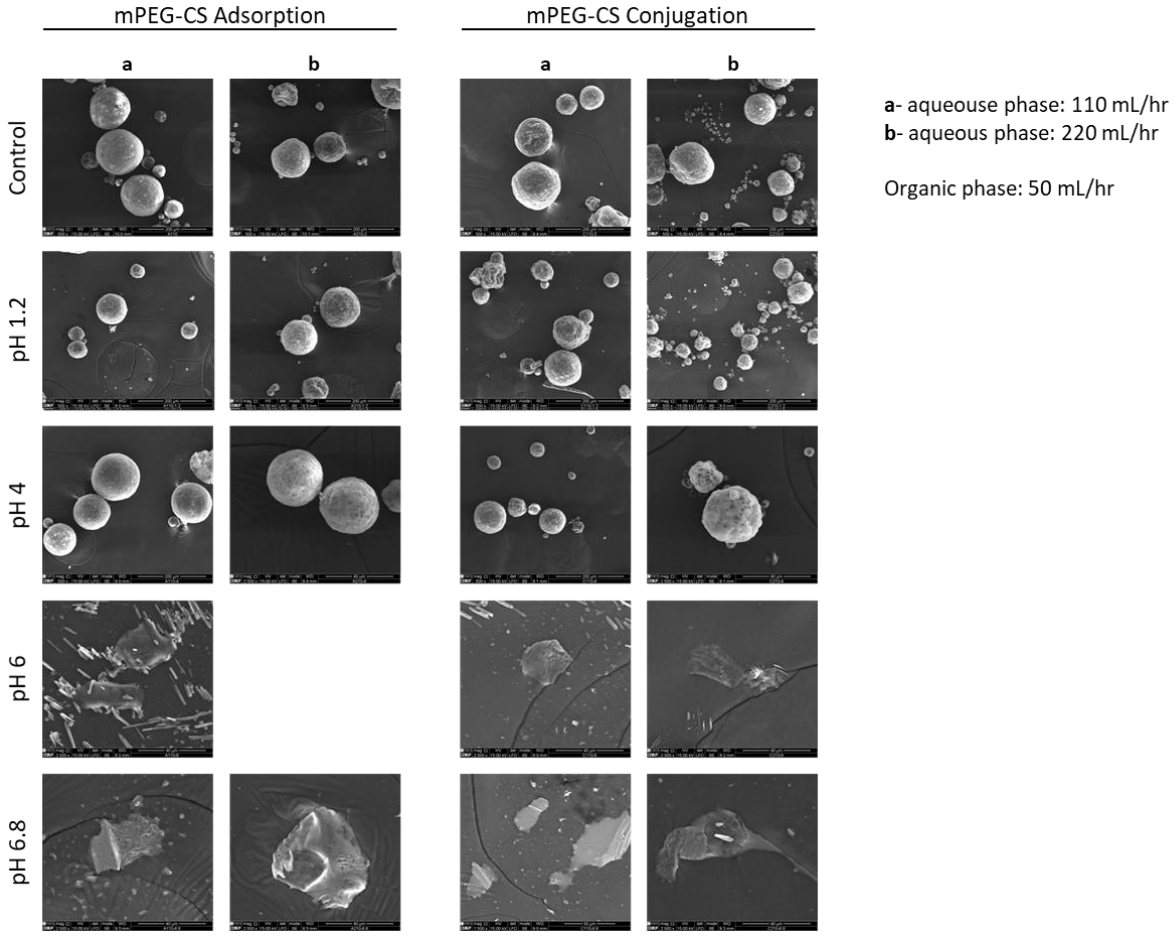

Fig. 21 *– SEM images of HPMC-AS microparticles, after 2h incubation with buffers with pH=1.2, 4. 6 and 6.8.*

Fig. 21 shows that using these parameters, the size of the MPs did indeed increase to around 100 µm. Nevertheless, polydispersion was still high as different sized populations were observable.

These formulations were used to assess the pH-responsive degradation of these MPs. After incubation with different pH solutions, we observed that MPs keep their structure in acidic environments (pH 1.2 and pH 4.0), but the HPMC-AS polymer degrades for pH 6.0 and pH 6.8. Thus, for oral delivery of Trp, these MPs seem to be able to provide a safe environment for the

encapsulated NPs by protecting them and the encapsulated molecule from the gastric milieu. The degradation should start occurring for pH=6.0, which better mimics the physiological conditions of small intestine, and where nanoparticles need to be exposed to the epithelium. In this experiment, MPs were also incubated with solutions of pH 5.5 however no MPs were observable neither was any degradation product. Due to over-accumulation of salts after evaporation of the buffer in these conditions, the obtained images were not conclusive and thus, this should be repeated for further validation of the results.

Chapter 5

CONCLUSIONS AND FUTURE WORK

5.1 Conclusions

The development of nanotechnology-based systems for the oral delivery of proteins is of great interest for pharmaceutical industry. Despite the low bioavailability of biomolecules when administered through this route, oral delivery is still the preferred via of administration due to high patience compliance. In this project, Triptorelin was used as a model peptide for the development of mucodiffusive and gastro-resistant Nanoparticle-in-Microparticle systems for oral delivery.

We were able to successfully encapsulate Triptorelin in PLGA NPs without significant alterations of the colloidal properties. Likewise, the conjugation with mPEG-CS of loaded NPs was also attained and within the values reported to confer mucodiffusing properties to the NPs.

When performing *in vitro* analysis, we observed that the mPEG-CS-PLGA NPs did not induce any further toxicity in the cell lines selected (Caco-2 and HT29MTX), when compared to the controls, thus suggesting the safety of the NPs produced. When assessing the permeation of the drug using relevant *in vitro* intestinal cell monolayers, the results were not as satisfying. The amount of triptorelin that crossed the membranes was very low which may be explained by the fact that the CS present in the formulation did not induce a transient opening of the tight-junctions as one would expect and also the releasing rate of the peptide from the drug did not occur as fast as desirable. The main conclusion to be drawn is that the NPs formulation needs optimization to act as a mucodiffusing system and to allow a faster release of the protein. Here, many parameters can be adjusted, namely the polymer used for NPs production or the substitution degree of PEG and/or CS conjugated to the NPs. Nevertheless, the assays conducted led to the conclusion that, with optimization, this system does indeed have potential to act as an alternative carrier for oral delivery of drugs currently administered through parenteral routes. More specifically the microencapsulation of the NPs proved to be efficient in protecting the encapsulated content from the acidic milieu of the stomach.

5.2 Future Work

Despite being a promising approach to the development of oral delivery formulations for peptides, many hurdles were detected along the way. Here, we were able to develop a gastroresistant system, but it did not present the mucodiffusive properties intended. Hence, future work has to address this problem, and develop new formulations to be tested *in vitro*. Some parameters that could be addressed at this stage would be the degree of modification of CS with PEG and the degree of substitution of mPEG-CS to PLGA NPs.

If no ratio presents satisfying results, then the production approach can be addressed, namely, the conjugation of the aforementioned polymers can be performed prior to NPs assembly, potentially promoting a less dense mesh in these systems, allowing a faster release of the drug. If this still proves to be inefficient, the final alternative would be developing this NiM systems using different polymers for the NPs formulations. Instead of PLGA, a different biodegradable polymer with a faster degradation rate could be selected.

After optimization of the final formulation, *in vitro* studies should be performed. More specifically, metabolic activity assays could be repeated but, this time, using fresh formulations. Permeability assays should also be repeated, but now with NPs dilution in a buffer that better mimics the physiological milieu, with the presence of enzymes for instance, that would likely accelerate the degradation of NPs polymers.

Both *in vitro* studies mentioned could be performed also for the NiM systems instead of just NPs formulations. Despite the fact that these systems will degrade at the intestinal epithelium, their degradation products will be in contact with the tissues, and thus may hamper cell activity or peptide permeation.

In a long term application and after all the required optimization already stated, these systems eventually could be tested *in vivo* and thus allow a better acknowledgment of its potentialities.

- this page was intentionally left in blank -

References

1. Zhang, L., et al., *Nanoparticles in medicine: therapeutic applications and developments.* Clinical pharmacology & therapeutics, 2008. **83**(5): p. 761-769.
2. Frokjaer, S. and D.E. Otzen, *Protein drug stability: a formulation challenge.* Nature reviews drug discovery, 2005. **4**(4): p. 298.
3. Mahato, R.I., et al., *Emerging trends in oral delivery of peptide and protein drugs.* Critical Reviews™ in Therapeutic Drug Carrier Systems, 2003. **20**(2&3).
4. Agasti, S.S., et al., *Nanoparticles for detection and diagnosis.* Advanced drug delivery reviews, 2010. **62**(3): p. 316-328.
5. Nikalje, A.P., *Nanotechnology and its applications in medicine.* Med chem, 2015. **5**(2): p. 185-189.
6. Chen, G., et al., *Nanochemistry and nanomedicine for nanoparticle-based diagnostics and therapy.* Chemical reviews, 2016. **116**(5): p. 2826-2885.
7. Bobo, D., et al., *Nanoparticle-based medicines: a review of FDA-approved materials and clinical trials to date.* Pharmaceutical research, 2016. **33**(10): p. 2373-2387.
8. Bhatia, S., *Nanoparticles types, classification, characterization, fabrication methods and drug delivery applications*, in *Natural Polymer Drug Delivery Systems*. 2016, Springer. p. 33-93.
9. Fakruddin, M., Z. Hossain, and H. Afroz, *Prospects and applications of nanobiotechnology: a medical perspective.* Journal of Nanobiotechnology, 2012. **10**: p. 31-31.
10. Morishita, M. and N.A. Peppas, *Is the oral route possible for peptide and protein drug delivery?* Drug discovery today, 2006. **11**(19-20): p. 905-910.
11. Zhang, L., et al., *Nanoparticles in medicine: therapeutic applications and developments.* Clinical pharmacology and therapeutics, 2008. **83**(5): p. 761-769.
12. Li, Y.-P., et al., *PEGylated PLGA nanoparticles as protein carriers: synthesis, preparation and biodistribution in rats.* Journal of Controlled Release, 2001. **71**(2): p. 203-211.
13. Shi, J., et al., *Nanotechnology in drug delivery and tissue engineering: from discovery to applications.* Nano letters, 2010. **10**(9): p. 3223-3230.
14. Mohanraj, V. and Y. Chen, *Nanoparticles-a review.* Tropical journal of pharmaceutical research, 2006. **5**(1): p. 561-573.
15. Zhang, L. and T.J. Webster, *Nanotechnology and nanomaterials: promises for improved tissue regeneration.* Nano today, 2009. **4**(1): p. 66-80.
16. Lee, S.H., et al., *Amine-functionalized gold nanoparticles as non-cytotoxic and efficient intracellular siRNA delivery carriers.* International journal of pharmaceutics, 2008. **364**(1): p. 94-101.
17. Huang, X., et al., *Gold nanoparticles: interesting optical properties and recent applications in cancer diagnostics and therapy.* 2007.
18. Malam, Y., M. Loizidou, and A.M. Seifalian, *Liposomes and nanoparticles: nanosized vehicles for drug delivery in cancer.* Trends in pharmacological sciences, 2009. **30**(11): p. 592-599.
19. Yang, Y., et al., *Self-assembly of size-controlled liposomes on DNA nanotemplates.* Nature chemistry, 2016. **8**(5): p. 476.

20. Singh, R. and J.W. Lillard Jr, *Nanoparticle-based targeted drug delivery.* Experimental and molecular pathology, 2009. **86**(3): p. 215-223.
21. Pridgen, E.M., F. Alexis, and O.C. Farokhzad, *Polymeric nanoparticle drug delivery technologies for oral delivery applications.* Expert opinion on drug delivery, 2015. **12**(9): p. 1459-1473.
22. Rathore, A.S., et al., *An Overview: Matrix Tablet as Controlled Drug Delivery System.* 2013.
23. Agrawal, U., et al., *Is nanotechnology a boon for oral drug delivery?* Drug discovery today, 2014. **19**(10): p. 1530-1546.
24. Goldberg, M. and I. Gomez-Orellana, *Challenges for the oral delivery of macromolecules.* Nature reviews Drug discovery, 2003. **2**(4): p. 289.
25. Donovan, M.D., G.L. Flynn, and G.L. Amidon, *Absorption of polyethylene glycols 600 through 2000: the molecular weight dependence of gastrointestinal and nasal absorption.* Pharmaceutical research, 1990. **7**(8): p. 863-868.
26. Thanou, M., J. Verhoef, and H. Junginger, *Oral drug absorption enhancement by chitosan and its derivatives.* Advanced drug delivery reviews, 2001. **52**(2): p. 117-126.
27. Emerich, D.F. and C.G. Thanos, *Targeted nanoparticle-based drug delivery and diagnosis.* Journal of drug targeting, 2007. **15**(3): p. 163-183.
28. Araújo, F.a.P., C. and Granja, PL and Santos, HA and Sarmento, B, *Functionalized nanoparticles for targeting the gastrointestinal apical membrane receptors*, in *Advances and Challenges in Oral Delivery of Macromolecules*. 2014, Future Medicine.
29. Ensign, L.M., R. Cone, and J. Hanes, *Oral drug delivery with polymeric nanoparticles: the gastrointestinal mucus barriers.* Advanced drug delivery reviews, 2012. **64**(6): p. 557-570.
30. Danhier, F., et al., *PLGA-based nanoparticles: an overview of biomedical applications.* Journal of controlled release, 2012. **161**(2): p. 505-522.
31. Panyam, J. and V. Labhasetwar, *Biodegradable nanoparticles for drug and gene delivery to cells and tissue.* Advanced drug delivery reviews, 2003. **55**(3): p. 329-347.
32. Semete, B., et al., *In vivo evaluation of the biodistribution and safety of PLGA nanoparticles as drug delivery systems.* Nanomedicine: Nanotechnology, Biology and Medicine, 2010. **6**(5): p. 662-671.
33. Vert, M., J. Mauduit, and S. Li, *Biodegradation of PLA/GA polymers: increasing complexity.* Biomaterials, 1994. **15**(15): p. 1209-1213.
34. Araújo, F., et al., *Safety and toxicity concerns of orally delivered nanoparticles as drug carriers.* Expert opinion on drug metabolism & toxicology, 2015. **11**(3): p. 381-393.
35. Ashford, M., *Gastrointestinal tract–physiology and drug absorption.* Aulton's Pharmaceutics E-Book: The Design and Manufacture of Medicines, 2017: p. 300-317.
36. Cone, R.A., *Barrier properties of mucus.* Advanced Drug Delivery Reviews, 2009. **61**(2): p. 75-85.
37. Meyer-Hoffert, U., et al., *Secreted enteric antimicrobial activity localises to the mucus surface layer.* Gut, 2008. **57**(6): p. 764-771.
38. Bevins, C.L. and N.H. Salzman, *Paneth cells, antimicrobial peptides and maintenance of intestinal homeostasis.* Nature Reviews Microbiology, 2011. **9**(5): p. 356.
39. Marieb, E.N., *Human anatomy & physiology*. 2001, San Francisco: Benjamin Cummings.
40. Mike Clark, M.D., *Smooth Muscle Excitation - Contraction*. 2016.
41. Mescher, A.L., *Junqueira's basic histology: text and atlas*. 2013: Mcgraw-hill.
42. Mohammed, M.A., et al., *An Overview of Chitosan Nanoparticles and Its Application in Non-Parenteral Drug Delivery.* Pharmaceutics, 2017. **9**(4): p. 53.
43. Lai, S.K., Y.-Y. Wang, and J. Hanes, *Mucus-penetrating nanoparticles for drug and gene delivery to mucosal tissues.* Advanced drug delivery reviews, 2009. **61**(2): p. 158-171.
44. Hamman, J.H., G.M. Enslin, and A.F. Kotzé, *Oral delivery of peptide drugs.* BioDrugs, 2005. **19**(3): p. 165-177.

45. Kumar Malik, D., et al., *Recent advances in protein and peptide drug delivery systems.* Current drug delivery, 2007. **4**(2): p. 141-151.
46. Giunchedi, P., et al., *Cellulose acetate trimellitate microspheres containing NSAIDs.* Drug development and industrial pharmacy, 1995. **21**(3): p. 315-330.
47. Pearnchob, N. and R. Bodmeier, *Dry polymer powder coating and comparison with conventional liquid-based coatings for Eudragit® RS, ethylcellulose and shellac.* European journal of pharmaceutics and biopharmaceutics, 2003. **56**(3): p. 363-369.
48. Tanno, F., et al., *Evaluation of hypromellose acetate succinate (HPMCAS) as a carrier in solid dispersions.* Drug development and industrial pharmacy, 2004. **30**(1): p. 9-17.
49. Shrestha, N., et al., *Multistage pH-responsive mucoadhesive nanocarriers prepared by aerosol flow reactor technology: A controlled dual protein-drug delivery system.* Biomaterials, 2015. **68**: p. 9-20.
50. Dong, Z. and D.S. Choi, *Hydroxypropyl methylcellulose acetate succinate: Potential drug–excipient incompatibility.* AAPs Pharmscitech, 2008. **9**(3): p. 991-997.
51. Zhang, H., et al., *Fabrication of a Multifunctional Nano-in-micro Drug Delivery Platform by Microfluidic Templated Encapsulation of Porous Silicon in Polymer Matrix.* Advanced Materials, 2014. **26**(26): p. 4497-4503.
52. Fallingborg, J., *Intraluminal pH of the human gastrointestinal tract.* Dan Med Bull, 1999. **46**(3): p. 183-96.
53. Atuma, C., et al., *The adherent gastrointestinal mucus gel layer: thickness and physical state in vivo.* American Journal of Physiology-Gastrointestinal and Liver Physiology, 2001. **280**(5): p. G922-G929.
54. Birchenough, G.M., et al., *New developments in goblet cell mucus secretion and function.* Mucosal immunology, 2015. **8**(4): p. 712.
55. Montagne, L., C. Piel, and J. Lalles, *Effect of diet on mucin kinetics and composition: nutrition and health implications.* Nutrition Reviews, 2004. **62**(3): p. 105-114.
56. Lehr, C.-M., et al., *An estimate of turnover time of intestinal mucus gel layer in the rat in situ loop.* International journal of pharmaceutics, 1991. **70**(3): p. 235-240.
57. Araújo, F., et al., *The impact of nanoparticles on the mucosal translocation and transport of GLP-1 across the intestinal epithelium.* Biomaterials, 2014. **35**(33): p. 9199-9207.
58. Lee, H.J., *Protein drug oral delivery: the recent progress.* Archives of pharmacal research, 2002. **25**(5): p. 572.
59. Serra, L., J. Doménech, and N.A. Peppas, *Engineering design and molecular dynamics of mucoadhesive drug delivery systems as targeting agents.* European journal of pharmaceutics and biopharmaceutics, 2009. **71**(3): p. 519-528.
60. Casettari, L., et al., *PEGylated chitosan derivatives: Synthesis, characterizations and pharmaceutical applications.* Progress in Polymer Science, 2012. **37**(5): p. 659-685.
61. Sogias, I.A., A.C. Williams, and V.V. Khutoryanskiy, *Why is chitosan mucoadhesive?* Biomacromolecules, 2008. **9**(7): p. 1837-1842.
62. Wang, Y., P. Li, and L. Kong, *Chitosan-modified PLGA nanoparticles with versatile surface for improved drug delivery.* Aaps Pharmscitech, 2013. **14**(2): p. 585-592.
63. Andrade, F., et al., *Chitosan formulations as carriers for therapeutic proteins.* Current drug discovery technologies, 2011. **8**(3): p. 157-172.
64. Smith, J., E. Wood, and M. Dornish, *Effect of chitosan on epithelial cell tight junctions.* Pharmaceutical research, 2004. **21**(1): p. 43-49.
65. Sonaje, K., et al., *Opening of epithelial tight junctions and enhancement of paracellular permeation by chitosan: microscopic, ultrastructural, and computed-tomographic observations.* Molecular pharmaceutics, 2012. **9**(5): p. 1271-1279.
66. Yamamoto, H., et al., *Surface-modified PLGA nanosphere with chitosan improved pulmonary delivery of calcitonin by mucoadhesion and opening of the intercellular tight junctions.* Journal of controlled Release, 2005. **102**(2): p. 373-381.

67. Amoozgar, Z., et al., *Low molecular-weight chitosan as a pH-sensitive stealth coating for tumor-specific drug delivery.* Molecular pharmaceutics, 2012. **9**(5): p. 1262-1270.
68. Netsomboon, K. and A. Bernkop-Schnürch, *Mucoadhesive vs. mucopenetrating particulate drug delivery.* European Journal of Pharmaceutics and Biopharmaceutics, 2016. **98**: p. 76-89.
69. Tobıo, M., et al., *The role of PEG on the stability in digestive fluids and in vivo fate of PEG-PLA nanoparticles following oral administration.* Colloids and Surfaces B: Biointerfaces, 2000. **18**(3-4): p. 315-323.
70. Bourganis, V., et al., *On the synthesis of mucus permeating nanocarriers.* European Journal of Pharmaceutics and Biopharmaceutics, 2015. **97**: p. 239-249.
71. Avgoustakis, K., *Pegylated poly (lactide) and poly (lactide-co-glycolide) nanoparticles: preparation, properties and possible applications in drug delivery.* Current drug delivery, 2004. **1**(4): p. 321-333.
72. Yu, T., et al., *Biodegradable mucus-penetrating nanoparticles composed of diblock copolymers of polyethylene glycol and poly (lactic-co-glycolic acid).* Drug delivery and translational research, 2012. **2**(2): p. 124-128.
73. Wang, Y.Y., et al., *Addressing the PEG mucoadhesivity paradox to engineer nanoparticles that "slip" through the human mucus barrier.* Angewandte Chemie International Edition, 2008. **47**(50): p. 9726-9729.
74. Schattling, P., et al., *A Polymer Chemistry Point of View on Mucoadhesion and Mucopenetration.* Macromolecular Bioscience, 2017.
75. Deshmukh, D., W.R. Ravis, and G.V. Betageri, *Delivery of didanosine from enteric-coated, sustained-release bioadhesive formulation.* Drug delivery, 2003. **10**(1): p. 47-50.
76. Lee, Y.-S., et al., *Production of nanoparticles-in-microparticles by a double emulsion method: A comprehensive study.* European Journal of Pharmaceutics and Biopharmaceutics, 2013. **83**(2): p. 168-173.
77. Tan, M.L., P.F.M. Choong, and C.R. Dass, *Recent developments in liposomes, microparticles and nanoparticles for protein and peptide drug delivery.* Peptides, 2010. **31**(1): p. 184-193.
78. Takeda, U., *Limited, Prostap 3 Leuprorelin acetate depot injection—summary of product characteristics.* URL: http://emc. medicines. org. uk/document. aspx.
79. Ward, K. and Z.H. Fan, *Mixing in microfluidic devices and enhancement methods.* Journal of Micromechanics and Microengineering, 2015. **25**(9): p. 094001.
80. Liu, D., et al., *Microfluidic-assisted fabrication of carriers for controlled drug delivery.* Lab on a Chip, 2017. **17**(11): p. 1856-1883.
81. Duncanson, W.J., et al., *Microfluidic synthesis of advanced microparticles for encapsulation and controlled release.* Lab on a Chip, 2012. **12**(12): p. 2135-2145.
82. Group, L.N.D., *Triptorelin & GnRH Analogues Review* London New Drugs Group, 2007.
83. Lundström, E.A., et al., *Triptorelin 6-month formulation in the management of patients with locally advanced and metastatic prostate cancer.* Clinical drug investigation, 2009. **29**(12): p. 757-765.
84. Smeets, J., *Timing of puberty-Which factors trigger pulsatile GnRH release and the onset of puberty?* 2015.
85. Donnez, J., et al., *Equivalence of the 3-month and 28-day formulations of triptorelin with regard to achievement and maintenance of medical castration in women with endometriosis.* Fertility and sterility, 2004. **81**(2): p. 297-304.
86. Prego, C., et al., *Chitosan–PEG nanocapsules as new carriers for oral peptide delivery: effect of chitosan pegylation degree.* Journal of Controlled Release, 2006. **111**(3): p. 299-308.
87. Holzer, M., et al., *Physico-chemical characterisation of PLGA nanoparticles after freeze-drying and storage.* European Journal of Pharmaceutics and Biopharmaceutics, 2009. **72**(2): p. 428-437.

88. Fonte, P., et al., *Stability study perspective of the effect of freeze-drying using cryoprotectants on the structure of insulin loaded into PLGA nanoparticles.* Biomacromolecules, 2014. **15**(10): p. 3753-65.
89. Araujo, F., et al., *Microfluidic assembly of a multifunctional tailorable composite system designed for site specific combined oral delivery of peptide drugs.* ACS nano, 2015. **9**(8): p. 8291-8302.
90. Lozoya-Agullo, I., et al., *Usefulness of Caco-2/HT29-MTX and Caco-2/HT29-MTX/Raji B Coculture Models To Predict Intestinal and Colonic Permeability Compared to Caco-2 Monoculture.* Molecular Pharmaceutics, 2017. **14**(4): p. 1264-1270.
91. Hubatsch, I., E.G. Ragnarsson, and P. Artursson, *Determination of drug permeability and prediction of drug absorption in Caco-2 monolayers.* Nature protocols, 2007. **2**(9): p. 2111.
92. Sarmento, B., *Concepts and Models for Drug Permeability Studies: Cell and Tissue Based in Vitro Culture Models*. 2015: Woodhead Publishing.
93. Liu, D., et al., *Microfluidic Assembly of Monodisperse Multistage pH-Responsive Polymer/Porous Silicon Composites for Precisely Controlled Multi-Drug Delivery.* Small, 2014. **10**(10): p. 2029-2038.
94. Martins, C.d.F., *Development of Polymeric Nanoparticles Loaded with Efavirenz Targeting Central Nervous System through Microfluidic Platforms*. 2017, Unversity of Porto. p. 107.
95. Kasaai, M.R., *Determination of the degree of N-acetylation for chitin and chitosan by various NMR spectroscopy techniques: A review.* Carbohydrate Polymers, 2010. **79**(4): p. 801-810.
96. Fulmer, G.R., et al., *NMR chemical shifts of trace impurities: common laboratory solvents, organics, and gases in deuterated solvents relevant to the organometallic chemist.* Organometallics, 2010. **29**(9): p. 2176-2179.
97. Li, X., et al., *Biodegradable MPEG-g-Chitosan and methoxy poly (ethylene glycol)-b-poly (ε-caprolactone) composite films: Part 1. Preparation and characterization.* Carbohydrate polymers, 2010. **79**(2): p. 429-436.
98. Liu, C.W. and W.J. Lin, *Polymeric nanoparticles conjugate a novel heptapeptide as an epidermal growth factor receptor-active targeting ligand for doxorubicin.* International Journal of Nanomedicine, 2012. **7**: p. 4749-4767.
99. Fulmer, G.R., et al., *NMR Chemical Shifts of Trace Impurities: Common Laboratory Solvents, Organics, and Gases in Deuterated Solvents Relevant to the Organometallic Chemist.* Organometallics, 2010. **29**(9): p. 2176-2179.
100. Mi, F.L., H.W. Sung, and S.S. Shyu, *Release of indomethacin from a novel chitosan microsphere prepared by a naturally occurring crosslinker: examination of crosslinking and polycation–anionic drug interaction.* Journal of Applied Polymer Science, 2001. **81**(7): p. 1700-1711.
101. Kong, X., et al., *Synthesis and characterization of a novel MPEG–chitosan diblock copolymer and self-assembly of nanoparticles.* Carbohydrate Polymers, 2010. **79**(1): p. 170-175.
102. Chakravarthi, S.S. and D.H. Robinson, *Enhanced cellular association of paclitaxel delivered in chitosan-PLGA particles.* International Journal of Pharmaceutics, 2011. **409**(1): p. 111-120.
103. Hung, H.-I., et al., *PLGA nanoparticle encapsulation reduces toxicity while retaining the therapeutic efficacy of EtNBS-PDT in vitro.* Scientific reports, 2016. **6**: p. 33234.
104. Gyulai, G., et al., *Preparation and characterization of cationic Pluronic for surface modification and functionalization of polymeric drug delivery nanoparticles.* Express Polymer Letters, 2016. **10**(3): p. 216.
105. Instruments, M., *Dynamic light scattering: an introduction in 30 minutes.* Technical Note Malvern, MRK656-01, 2012: p. 1-8.

106. Filipe, V., A. Hawe, and W. Jiskoot, *Critical evaluation of Nanoparticle Tracking Analysis (NTA) by NanoSight for the measurement of nanoparticles and protein aggregates.* Pharmaceutical research, 2010. **27**(5): p. 796-810.
107. Parveen, S. and S.K. Sahoo, *Long circulating chitosan/PEG blended PLGA nanoparticle for tumor drug delivery.* European journal of pharmacology, 2011. **670**(2-3): p. 372-383.
108. ISO, I., *10993–5: 2009 Biological Evaluation of Medical Devices–Part 5: Tests for in Vitro Cytotoxicity.* International Organization for Standardization, Geneva, 2009.
109. Nollevaux, G., et al., *Development of a serum-free co-culture of human intestinal epithelium cell-lines (Caco-2/HT29-5M21).* BMC cell biology, 2006. **7**(1): p. 20.
110. Hilgendorf, C., et al., *Caco-2 versus caco-2/HT29-MTX co-cultured cell lines: permeabilities via diffusion, inside-and outside-directed carrier-mediated transport.* Journal of pharmaceutical sciences, 2000. **89**(1): p. 63-75.
111. Volpe, D.A., *Variability in Caco-2 and MDCK cell-based intestinal permeability assays.* Journal of pharmaceutical sciences, 2008. **97**(2): p. 712-725.
112. Meaney, C. and C. O'Driscoll, *Mucus as a barrier to the permeability of hydrophilic and lipophilic compounds in the absence and presence of sodium taurocholate micellar systems using cell culture models.* European journal of pharmaceutical sciences, 1999. **8**(3): p. 167-175.